Feeder-free culture of naive human pluripotent stem cells retaining embryonic, extraembryonic and blastoid generation potential

Giada Rossignoli[1,#], Michael Oberhuemer[2,3,#], Ida Sophie Brun[4,#], Irene Zorzan[1,15,#], Anna Osnato[5,6], Anne Wenzel[4], Emiel van Genderen[7], Andrea Drusin[1], Giorgia Panebianco[1], Nicolò Magri[1], Mairim Alexandra Solis[5,8], Chiara Colantuono[9], Sam Samuël Franciscus Allegonda van Knippenberg[5,6], Thi Xuan Ai Pham[5,6], Sherif Khodeer[5,6], Paolo Grumati[10,11], Davide Cacchiarelli[10,12,13], Paolo Martini[14], Nicolas Rivron[7], Vincent Pasque[5,6], Jan Jakub Żylicz[4,*], Martin Leeb[2,*] and Graziano Martello[1,*].

Affiliations

1: Department of Biology, University of Padua, Padua, Italy.
2: Max Perutz Laboratories Vienna, University of Vienna, Vienna BioCenter, Vienna, Austria.
3: Vienna BioCenter PhD Program, Doctoral School of the University of Vienna, Medical University of Vienna, Vienna, Austria.
4: Novo Nordisk Foundation Center for Stem Cell Medicine, reNEW, University of Copenhagen, Copenhagen, Denmark.
5: KU Leuven-University of Leuven, Department of Development and Regeneration, Leuven Stem Cell Institute, Leuven, Belgium.
6: KU Leuven Institute for Single Cell Omics (LISCO), Leuven, Belgium.
7: Institute of Molecular Biotechnology of the Austrian Academy of Sciences (IMBA), Vienna BioCenter, Vienna, Austria
8: Gorgas Memorial Institute for Health Studies, Panama, Panama.
9: NEGEDIA S.r.l., Pozzuoli, Italy.
10: Telethon Institute of Genetics and Medicine (TIGEM), Pozzuoli, Italy.
11: Department of Clinical Medicine and Surgery, University of Naples "Federico II", Naples, Italy.
12: Department of Translational Medicine, University of Naples "Federico II", Naples, Italy.
13: Genomics and Experimental Medicine Program, Scuola Superiore Meridionale (SSM, School of Advanced Studies), Naples, Italy.
14: Department of Molecular and Translational Medicine, University of Brescia, Brescia, Italy.
15: Current affiliation: Epigenetics Programme, Babraham Institute, Cambridge, UK.

[#]equal contributions; *Corresponding authors

Abstract

Conventional human pluripotent stem cells (hPSCs) are widely used to study early embryonic development, generate somatic cells, and model diseases, with differentiation potential aligned to a post-implantation epiblast identity. In the past decade, naive hPSCs, representing a pre-implantation stage, have been derived. Naive hPSCs efficiently differentiate towards embryonic and extraembryonic lineages such as trophectoderm, primitive endoderm, and extraembryonic mesoderm, and also self-organize into blastocyst-like structures called blastoids. However, their culture typically relies on mouse embryonic fibroblasts (MEFs), which are variable, resource-intensive, and can confound analyses. We report the long-term maintenance of naive hPSCs in a feeder-free, serum-coated system. We successfully expanded for up to 25 passages 8 different naive hPSCs lines across 5 laboratories. Growth rate, clonogenicity, and gene expression profiles on serum coating were comparable to MEF-based cultures, but serum coating eliminated fibroblast contamination. Naive hPSCs cultured on serum exhibited more efficient germ layer specification, retained trophectoderm potential and high blastoid formation efficiency. Exome sequencing revealed fewer mutations in serum-cultured cells, and mass spectrometry identified extracellular matrix proteins such as vitronectin, fibronectin, and collagens in the serum coating. Overall, serum coating offers a scalable, cost-effective and therefore widely applicable alternative for naive hPSC culture, maintaining developmental potential, reducing DNA mutations, and eliminating MEF-related confounding factors. We believe serum coating will expand the use of naive hPSCs to large-scale studies and facilitate the investigation of mechanistic insights into developmental and disease modelling.

Keywords:

Naive pluripotency; blastoids; extraembryonic lineages, extracellular matrix.

Introduction

The derivation of human pluripotent stem cells (hPSCs) has transformed the stem cell field. Given their potential to self-renew and differentiate into specialised cell types, there have been high expectations for their use in biological and medical research. hPSCs were first derived from the inner cell mass (ICM) of *in vitro* fertilised embryos (Human Embryonic Stem Cells, hESCs), and cultured in serum-based media on a feeder layer of inactivated mouse embryonic fibroblasts (MEFs)[1], following the methods developed for ICM-derived mouse ESCs (mESCs)[2]. However, it soon became clear that the self-renewal requirements of hESCs and mESCs were different. Undifferentiated mESCs could be maintained in feeder-free conditions in the presence of leukaemia inhibitory factor (LIF) and foetal bovine serum (FBS) on gelatin-coated plates[3,4]. Subsequently, two inhibitors (2i), the MEK inhibitor PD0325901 and the GSK3 inhibitor CHIR99021 were shown to promote efficient mESCs self-renewal in the absence of feeders[5,6]. The combination of 2i and the cytokine LIF (2iL) resulted in more robust proliferation, increased oxidative phosphorylation and genome hypomethylation[7–9]. Since 2007, when hPSCs were reprogrammed from human somatic cells (human induced pluripotent stem cells, hiPSCs) by overexpressing a cocktail of transcription factors (OCT4, SOX2, KLF4 and c-MYC from Takahashi *et al*[10], and OCT4, SOX2, NANOG and LIN28 from Yu *et al*[11]), hundreds of lines of hPSCs have been derived. Surprisingly, hPSCs were found not responsive to 2iL[12]. In contrast, they can be cultured without feeders on Matrigel or vitronectin-coated plates in Essential 8 (E8) or mTeSR media, both based on FGF2 and TGFβ supplementation[13–15].

Although hESCs, like mESCs, are derived from pre-implantation blastocysts, they do not reside in a naive state of pluripotency and rather correspond to primed mouse ESCs derived from post-implantation epiblast (mEpiSCs), regarding growth factor dependence and transcriptional and epigenetic regulation[16–19]. Furthermore, hESCs (and hiPSCs) exhibit lower expression of pluripotency genes such as *NANOG*, *KLF4*, *KLF17*, *DPPA3*, and *DPPA5* when compared to the human naive epiblast[20]. The ability to convert mEpiSCs into mESCs provided a paradigm for the generation of naive human stem cells. This led different research groups to first derive naive hPSCs in 2iL by overexpressing transcription factors associated with naive pluripotency[12,21], and later to implement more specific culture conditions and genetic manipulations[22–25]. Since then, naive hPSCs have been successfully derived from human blastocysts and somatic cell reprogramming by transient gene overexpression or chemical resetting from primed hPSCs in various media[26–30]. Successful maintenance of human naive pluripotency *in vitro* in a transgene-independent manner and in serum-free medium was initially achieved by culture optimisation starting from 2iL conditions[24,25]. The addition of Gö6983, a protein kinase C (PKC) inhibitor, previously shown to suppress also mESCs differentiation[31], combined with a lower concentration of CHIR99021 (t2iLGö) was beneficial in maintaining compact colonies with morphology and proliferation of naive hESCs[24]. Later on, GSK3 inhibition was shown to be dispensable

for the maintenance and resetting of naive hPSCs, so CHIR99021 was omitted and the tankyrase inhibitor XAV939 (PXGL) was added to achieve more robust and stable naive features[32]. A high-throughput chemical screen identified a combination of compounds, including the alternative GSK3 inhibitor IM12, the BRAF inhibitor SB590885, the SRC inhibitor WH-4-023, and the ROCK inhibitor Y-27632, supplemented with FGF and Activin A that synergise with PD0325901 and LIF to support the expansion of naive hPSCs (5i/L/AF)[25]. The addition of the JNK inhibitor SP600125 (6i/L/A) has been reported to increase the efficiency of naive hPSCs induction from the primed state[25]. Meanwhile, chemically defined conditions termed NHSM (naive human stem cell medium) were developed, in which 2iLGö was supplemented with p38 inhibitor SB203580 or BIRB796, JNK inhibitor SP600125, ROCK inhibitor Y-27632, bFGF and TGF-β1[23].

The derivation of naive hPSCs has broadened the potential applications of human embryonic stem cells. Consistent with the fact that their transcriptomic state reflects a developmental state similar to the blastocyst stage epiblast rather than post-implantation epiblast, naive hPSCs exhibit a broader differentiation potential compared to primed hPSCs, enabling efficient differentiation into extraembryonic tissues, including trophectoderm (TE)[33–36], primitive endoderm (PrE)[37,38], and extraembryonic mesoderm[39], three lineages previously inaccessible for *in vitro* studies. Furthermore, naive hPSCs can aggregate and generate 3D blastocyst-like structures composed of the three founding lineages as a model to study human implantation and peri-implantation development[40–42]. Naive hPSCs are characterised by global genomic hypomethylation compared to primed cells[43] - like mESCs[9] - and biallelic expression of multiple imprinted genes[44,45]. Naive hPSCs also use a bivalent metabolic system with a greater reliance on oxidative metabolism, whereas primed hPSCs are almost exclusively glycolytic[24,25,46,47], as reported for naive mESCs[8].

A major hurdle for studying the human naive state is that, unlike the mouse naive and human primed states, they are still routinely cultured on MEFs. In addition to the experimental cost and time involved, the quality of culture on feeders has been shown to depend on numerous other factors such as embryo age, passage number of MEFs and their genetic background, all of which affect gene expression and factor release from MEFs themselves, as well as stem cells proliferation and colony formation[48–51]. The exchange of signals between feeders and PSCs, some of which are still unknown, undoubtedly prevents a stringent control of the system and makes it more difficult to understand the best conditions and underlying biological pathways necessary for maintaining pluripotency *in vitro*, with implications also in downstream analyses and applications of these cells. There have been extensive efforts to eliminate feeders from naive hPSC cultures. However, to this date, they have not been widely adopted for multiple reasons. A 3D culture system based on Matrigel allows for a robust expansion of naive hPSCs in PXGL[52]. While it allows for efficient 3D differentiation, it is time- and resource-intensive as a routine culture method. Reduced proliferation was reported if MEFs were replaced with Matrigel or laminin-511 coating in t2iLGö medium in 2D[24]. Media formulations with extensive addition of inhibitors

130 allowed for robust expansion of hPSCs on Matrigel or Vitronectin-coated plates (FINE, NHSM and
131 RSeT, a commercial medium based on NHSM)[23,53]. However, these inhibitors affect the morphology[53]
132 or stabilise a transcriptional state of hPSCs distinct from naive cells routinely used in blastoid
133 formation[23,27]. Consequently, the routinely used conditions for naive hPSCs expansion and blastoid
134 generation rely on MEFs[40–42].

135 The addition of serum to cell culture media has been used to improve cell adhesion since the first half
136 of the last century[54–56]. Analysis of serum composition led to the discovery of the extracellular matrix
137 (ECM) protein vitronectin[57], together with fibronectin[58]. Murine EpiSCs can be expanded efficiently on
138 FBS-coated plates[16]. Interestingly, mESCs cultured on serum-coated substrates in the presence of LIF
139 maintain the expression of *OCT4* and grow as round cells in small colonies[59]. Moreover, while mESCs
140 strongly attach when converted from 2iL to serum/LIF, cells in a serum-containing medium might have
141 attachment problems when converted to serum-free 2iL, and the addition of a small amount of FBS in
142 2iL generally enhances adhesion[60]. Furthermore, conventional hPSCs have been successfully grown on
143 serum-coated substrates without feeders[61].

144 In this study, we observed, across 5 laboratories, that naive hPSCs of both induced and embryonic
145 origins can be easily adapted to a feeder-free, serum-based coating in PXGL. Cells grown on serum
146 coated culture dishes retain a naive pluripotency gene expression signature, and a proliferation rate and
147 clonogenic capacity similar to the original lines on MEFs, without acquiring pathogenic-associated
148 mutations. In addition, naive hPSCs cultured on serum coating retain full differentiation potential
149 towards both extra-embryonic and embryonic tissues as well as the capacity to self-assemble into
150 blastoids.

151 # Results

152 ## Naive hPSCs spontaneously adapt to serum coating

153 Naive hiPSCs directly reprogrammed from somatic cells[30] were plated in PXGL medium on dishes
154 coated with 10% FBS diluted in DMEM (i.e. serum coating) without MEFs. Feeder-free converted cells
155 retained their distinctive dome-shaped morphology (Supplementary Figure 1A) and expressed general
156 pluripotency (*POU5F1/OCT4* and *NANOG*) and naive-specific markers (*TFCP2L1*, *KLF4* and *KLF17*)
157 at comparable or even higher levels than cells cultured on MEFs, as well as low or undetectable
158 expression of primed genes *OTX2* and *ZIC2* (Figure 1A). Comparable protein levels of naive markers
159 KLF17 and TFCP2L1, and of the general pluripotency markers OCT4 and NANOG were observed in
160 feeder-free and MEFs cultured cells (Figure 1B, left, and Supplementary Figure 1B). Two naive PSC
161 lines (HPD06 and HPD03) displayed a decrease in the proliferation rate (Supplementary Figure 1D)
162 and clonogenic capability (Supplementary Figure 1E) when plated at low density on serum coating in
163 comparison to the same cell lines on MEFs during the first 4 passages of the conversion. Upon long-
164 term culture in feeder-free conditions, these hPSC lines retained the dome-shaped morphology (Figure
165 1C, left) and recovered growth rate and clonogenicity to levels comparable to the same cell line cultured
166 on MEFs (Figure 1D-E). We conclude that serum coating allows for the maintenance of naive
167 pluripotency markers and the long-term expansion of naive hiPSCs.

168 Prompted by these results, we decided to test extensively whether serum coating could be used for naive
169 PSC lines of different origin (i.e. reprogramming of fibroblasts, resetting of conventional PSCs and
170 embryo-derived), of both sexes and in different laboratories. Furthermore, we reasoned that an extensive
171 test of the differentiation potential should be performed, including both embryonic and extraembryonic
172 lineages, to test if serum coating allows for the maintenance of *bona fide* naive PSCs (Figure 1F). We
173 successfully converted 8 human naive PSC lines in 5 different laboratories to feeder-free conditions
174 (Table 1). They all displayed comparable expression of nuclear (OCT4 and NANOG) and naive markers
175 (KLF17 and SUSD2) (Figure 1B, G and Supplementary Figure 1C), with dome-shaped morphology
176 and robust expansion (Figure 1C). Although only HPD06 and HPD03 lines exhibited a lag phase before
177 complete adaptation, we have not experienced a line failing to convert to serum coating in PXGL.

178 We concluded that naive hPSCs spontaneously adapt to the feeder-free culture on serum coating in
179 PXGL without additional treatment or genetic manipulation.

180 ## Proteomics analysis of serum composition reveals abundant ECM proteins

181 We wondered how serum coating could sustain the attachment and growth of naive hPSCs. Previous
182 studies identified Vitronectin as a component of serum accounting for its capacity to promote cell

183 adhesion[57]. Therefore we assessed the composition of the coating through a label-free quantitative
184 proteomics analysis. The entire list of identified proteins was screened and annotated for matrisome and
185 matrisome-associated macromolecules using the Matrisome AnalyseR tool from The Matrisome
186 Project[62]. Of the 850 proteins detected in serum coating, 183 (more than 20%) were classified as "Core
187 matrisome" or "Matrisome-associated" hits. ECM glycoproteins and ECM-affiliated proteins and
188 regulators accounted for the majority of the hits in these two categories (Figure 2A). The analysis of the
189 top 100 most prevalent proteins in serum coating showed that Fibronectin, Vitronectin, Laminin, and
190 several Collagens were present (Figure 2B).

191 Therefore, the serum contains a mixture of ECM proteins previously reported to support conventional
192 human PSCs[13–15].

193 Serum coating does not induce genetic variations in naive hPSCs

194 Several studies demonstrated that conventional hPSCs can acquire genetic changes during long-term *in*
195 *vitro* culture, which commonly include mutations in cancer-associated genes, especially TP53[63,64]. We
196 analysed specifically the two naive iPSC lines (HPD06 and HPD03) that required some passages to
197 recover their proliferation rate on serum (Figure 1D), wondering whether they acquired mutations in
198 hotspot genes during the adaptation. We collected genomic DNA from HPD06 and HPD03 cultured for
199 more than 2 months after conversion to serum coating and from the same lines kept on MEFs (Figure
200 3A) and deep sequenced exomes (more than 600 million reads, 1000x independent base coverage). The
201 comparison with the reference genome identified a total of 1649 shared variants (SNVs, indels, and
202 CNVs) in protein-coding regions between HPD06 naive hPSCs cultured on MEFs and serum, likely
203 accumulated during derivation and previous culture on MEFs (Figure 3B, left Venn diagrams).
204 However, HPD06 continuously cultured on MEFs accumulated 936 variants, contrary to the 356
205 variants specifically detected in the same line cultured on serum. Similarly, more variants were detected
206 in HPD03 naive hPSCs on MEFs than in the same line converted to serum coating (509 and 311,
207 respectively; Figure 3B, top Venn diagrams). We then grouped protein-coding variants according to
208 their clinical impact (tier I, strong significance; tier II, potential clinical significance; tier III, unknown
209 clinical significance; and tier IV, benign or likely benign)[65]. For both HPD06 and HPD03, no Tier I
210 alterations were identified and Tier IV represented the vast majority of detected variants (Figure 3B,
211 bottom bar plots). Interestingly, for both naive lines, the culture on MEFs showed an accumulation of
212 Tier III variants compared to serum coating (Figure 3B, bar plots). Few cancer-related genes previously
213 reported as commonly mutated in conventional hPSCs showed only Tier IV benign or likely benign
214 alterations (*FAT1*, *ASXL1* and *NF1*)[64]. No genetic alteration was found for *TP53*, a predominantly
215 mutated gene during *in vitro* culture[63,64].

216 Overall, culturing naive hPSCs on serum coating did not lead to pathogenic mutations. Moreover,
217 mutation rates of naive lines cultured on serum were lower compared to MEFs-cultured cells.

218 Naive hPSCs on serum coating maintain the transcriptomic profile and lack
219 of gene imprinting

220 To further characterise the naive features of hPSCs on serum, we compared the transcriptome of our
221 naive hPSCs cultured on MEFs and serum coating with a panel of published transcriptomes spanning
222 human naive and primed PSCs, TSCs and fibroblasts. RNA-seq data confirmed a distinct global
223 expression profile of our naive hPSC lines compared with primed hPSCs, TSCs and fibroblasts, as they
224 fall together within the main naive cluster (Figure 3C). Gene expression analysis confirmed robust
225 induction of several core and naive specific pluripotency genes (Figure 3D), and low to undetectable
226 expression of primed-specific markers, in line with published transcriptomes. Generally, primed and
227 naive hPSCs cultured on MEFs showed variable expression of fibroblast markers, possibly due to MEF
228 contamination in collected cells (Figure 3D and Supplementary 2C). Fibroblast markers were barely
229 detectable in naive lines cultured on serum.

230 It has been observed that mitochondrial activation and metabolic realignment occur concurrently with
231 the generation and stabilisation of naive hPSCs[24]. Mouse ESCs use oxidative phosphorylation, while
232 mEpiSCs and hPSCs are mostly glycolytic and have a low ability for mitochondrial respiration[46]. We
233 collected the list of oxidative phosphorylation genes from KEGG (ko00190 pathway;
234 https://www.genome.jp/kegg/pathway.html) and added the complex IV cytochrome c oxidase (COX)
235 genes. In naive hPSCs, we observed an increase in the expression of most genes involved in oxidative
236 phosphorylation (Supplementary Figure 2A). Furthermore, in agreement with previously published
237 data[24,46], the expression of most of the COX genes was decreased in primed hPSCs compared to naive
238 hPSCs, both on MEFs and serum coating.

239 Previous studies reported biallelic expression of some imprinted genes in human naive PSCs[44,45,66].
240 Therefore, we analysed our bulk RNA-Seq samples with BrewerIX[45], running the analysis with the
241 complete pipeline. We detected a significant biallelic expression of H19 and ZIM2/PEG3 specifically
242 in all naive hiPSCs, either on serum or MEFs, but not in primed hiPSCs (Supplementary Figure 2B), as
243 previously reported[44,67]. Overall, naive cells displayed similar allelic expression of imprinted genes on
244 serum and MEFs.

245 We concluded that naive hPSCs cultured on serum coating maintain their distinctive transcriptome
246 profile without significant alterations compared to naive hPSCs cultured on MEFs.

247 **Serum-adapted naive hPSCs faithfully recapitulate embryonic**
248 **differentiation trajectories**

249 Upon withdrawal of self-renewal cues, naive hESCs exit the naive pluripotent state. Before gaining the
250 ability to commit to embryonic cell fates, they need to undergo a process termed capacitation[68].
251 Capacitation requires approximately eight to ten days, consistent with the timing between the blastocyst
252 and the pre-gastrulation post-implantation embryo *in vivo*. Hence, to assess the capacitation and
253 differentiation potential of serum-cultured naive hPSCs (Figure 1F), we subjected them to a variety of
254 differentiation conditions. Changes in morphology were equivalent between naive hPSCs cultured on
255 MEFs or serum coating, across multiple differentiation media (Supplementary Figure 3A). Furthermore,
256 expression of naive specific markers (*TFCP2L1*, *KLF4* and *NANOG*) was downregulated while
257 expression of primed markers (*SALL2*, *CDH2* and *ZIC2)* was induced during the exit from naive
258 pluripotency irrespective of whether hESCs were maintained on MEFs or serum before the induction
259 of differentiation (Figure 4A). Consistently, naive transcription factors downregulation and primed
260 marker upregulation were also observed in Shef6 hESCs cultured on serum coating inducing
261 capacitation (Figure 4B) and were confirmed at the protein level (Supplementary Figure 3B).

262 To further characterise gene expression behaviour during capacitation, we explored transcriptome
263 changes throughout an eight-day differentiation time course in various conditions: unsupplemented
264 N2B27, N2B27 supplemented with TNKS1/2 inhibition (XAV)[68] or FGF2-ActivinA-XAV (FAX), or
265 E8 or mTeSR, which contain FGF and Activin signalling ligands. All differentiation was induced from
266 naive Shef6 hESCs cultured on serum. We firstly noted that differentiation time points, rather than
267 medium conditions, had the largest impact on clustering (Figure 4C) and that the Spearman correlation
268 between the same time points of different conditions was high (Supplementary Figure 3C).
269 Consistently, expression kinetics of *KLF4* and *ZIC2* were equivalent between conditions (Figure 4D).
270 Comparison with published data for MEF-cultured H9 and HNES1 naive hESC lines differentiating
271 with XAV[68], showed that Shef6 naive hESCs cultured on serum coating followed the same trajectory
272 as H9 and HNES1 hESCs cultured on MEFs before capacitation (Figure 4E), and have similar
273 expression patterns for known pluripotency genes (Figure 4F). We also noted that the presence of XAV
274 had no discernable effect regarding gross gene expression or proliferation compared to capacitation in
275 N2B27 alone. We surmise that the gene expression programme accompanying capacitation is not
276 affected by the substrate used for culture.

277 We next benchmarked our *in vitro* capacitation system starting from serum-coated naive hPSCs by
278 comparing our RNA-seq time course data to data of human *ex vivo* cultured pre- and peri-implantation
279 embryos[69]. Principal component analysis showed a striking alignment between our *in vitro* capacitation
280 system and embryo data (Figure 4G). This is reflected in a clear correlation between differentiation-

281 induced gene expression changes *in vitro* and *in vivo* at both the global transcriptome (Supplementary
282 Figure 3D), and the individual pluripotency marker level (Figure 4F and Supplementary Figure 3E-F).

283 Taken together, these findings demonstrate that serum-adapted hPSCs progress through the
284 developmental states of pluripotency at least as well as feeder-dependent hPSCs and that this model can
285 generate results compatible with *in vivo* embryonic development.

286 Naive hPSCs on serum coating efficiently differentiate to the three primary 287 germ layers and TSCs

288 After confirming that naive hPSCs cultured on serum can exit pluripotency under different conditions
289 with a progression similar to that of the same cell line cultured on MEFs (Figure 4 and Supplementary
290 Figure 3), we wondered if naive hPSCs cultured in feeder-free conditions still retain the capacity to
291 efficiently differentiate into embryoid bodies (EBs) composed of the three germ layers (Figure 1F).
292 Capacitated hPSCs from naive cells previously cultured on MEFs or serum coating were aggregated in
293 3D and let spontaneously differentiate for 14 days (Figure 5A). EBs derived from both conditions
294 showed an upregulation of germ layer markers compared to capacitated cells (Figure 5B). We conclude
295 that naive hPSCs cultured on serum efficiently capacitate and differentiate to the three germ layers with
296 similar or even better efficiency compared to naive hPSCs previously cultured on MEFs.

297 Naive hPSCs cultured on MEFs can also promptly differentiate toward TSCs when exposed to TSC
298 medium[34,35,70]. Therefore, we assessed whether naive hPSCs cultured on serum coating still retain this
299 capacity. We obtained TSCs in a few passages from naive hiPSCs stably cultured in both conditions,
300 which showed indistinguishable morphology (Figure 4C) and similar downregulation of naive genes
301 *TFCP2L1* and *KLF17* and upregulation of TSC genes *GATA3* and *GATA2* (Figure 5D and
302 Supplementary Figure 4A). Consistently, the GATA3 signal was detected by immunofluorescence at a
303 comparable level to stable naive-derived TSCs (passage 15), while KLF17 and OCT4 were undetectable
304 (Figure 5E and Supplementary Figure 4B). Several genes (e.g. *TFAP2A*, *KRT7,* and *GATA3* and *GATA2*
305 to a lesser extent) are shared between TSCs and amnion, as early amniogenesis has been reported to
306 occur via a trophectoderm-like route[71]. Therefore, we wondered if TSCs derived from naive hiPSCs
307 cultured on serum retain the same low expression of amnion markers of naive hiPSCs cultured on MEFs.
308 We previously reported that BAP medium-treated primed hPSCs showed increased expression of
309 *GATA3* together with amnion markers *IGFBP3* and *BAMBI*[72]. Therefore, we exposed primed
310 Keratinocytes induced Pluripotent Stem Cells (KiPS) to BAP medium and observed a cell morphology
311 consistent with previous reports[36,72,73] and completely distinct from our naive hiPSCs-derived TSCs
312 (Supplementary Figure 4C, left and Figure 4A). We analysed the expression of the amnion markers[35,70]
313 and detected lower expression of *IGFBP3* and undetectable expression of *BAMBI* in TSCs derived from
314 naive hiPSCs cultured both on MEFs and serum coating compared to BAP-treated cells (Supplementary

315 Figure 4C). We concluded that naive hiPSCs cultured in both conditions readily differentiate to *bona*
316 *fide* TSCs with similar efficiency.

317 Naive hPSCs on serum coating efficiently self-organize into blastoids

318 Previous studies have reported that naive hPSCs when aggregated are able to self-organize into
319 blastoids. Blastoids are integrated stem cell embryo models reminiscent of the human blastocyst[40–42].
320 Indeed, such structures robustly specify an outer layer of TE-like cells encompassing the pluripotent
321 epiblast (EPI)-like cells and rare PrE-like cells. To test if naive hPSCs cultured on serum retain this
322 unique characteristic, we optimised the Kagawa *et al*[41,74] blastoid induction protocol for naive H9 hESCs
323 (Table 1). When passaged at high densities, naive H9 hESCs cultured on serum coating were able to
324 aggregate in AggreWells and form blastoid structures without the need for the time-consuming plastic
325 attachment step typically used to deplete MEFs and differentiated cells from the cultures (Figure 6A,
326 top). Blastoids derived from naive H9 hESCs cultured on serum coating showed comparable cavitation
327 efficiency, diameter, and rate of single cavities to blastoids derived from naive hESCs cultured on
328 feeders (Figure 6A, top and Supplementary Figure 5A). Comparable efficiency of blastoid formation
329 was observed also using the male naive hiPSC line KOLF2.1J cultured on MEFs or on serum coating
330 (Figure 6A, bottom). Immunofluorescence analysis validated that these structures contain TE-like
331 (GATA2/3 or CDX2), EPI-like (NANOG or OCT4), and rare PrE-like cells (GATA4 and SOX17)
332 (Figure 6B). Comparable results were obtained with naive HNES1 hESCs and the female naive hiPSC
333 line SCTi003-A (Supplementary Figure 5B-C). This analysis confirmed that naive hESCs and hiPSCs
334 cultured on serum-coated dishes are able to robustly self-organize into blastoids.

335 To validate these cellular identities, we performed 10x scRNAseq on day 5 blastoids derived from naive
336 H9 hESCs cultured on serum-coated dishes. This analysis showed two populations of cells on the
337 UMAP (Figure 6C). Based on the expression of key marker genes, the two populations were annotated
338 as TE-like and EPI-like cells (Figure 6D-E). Notably, TE-like cells expressed a wide range of
339 trophoblast markers (e.g., *GATA3, NR2F2, GATA2*) but not those of the amnion (e.g., *ISL1, TFAP2B*)
340 or other off-target lineages (Figure 6D-E, Supplementary Figure 5D). Similarly, EPI-like cells
341 expressed both core (e.g., *POU5F1, NANOG*) and naive pluripotency markers (e.g., *DPPA5, DNMT3L*)
342 but not those associated with primed pluripotency (e.g., *OTX2, ZIC2*) (Figure 6D-E, Supplementary
343 Figure 5D). Previous reports have shown that PrE-like cells are very rarely specified during blastoid
344 induction[41]. Consistent with this finding, we only observed sporadic individual cells expressing the PrE
345 marker *GATA4*, and no Seurat cluster contained a significant number of PrE-like cells (Supplementary
346 Figure 5D-E). To further validate these annotations, we integrated our data with embryo reference
347 datasets (Supplementary Figure 5F)[20,40,69,75–78]. Notably, our single-cell dissociation protocol
348 disproportionately fragilizes the TE-like cells; therefore, scRNA-seq was only used to verify cellular
349 identities rather than to quantify the proportion of individual lineages. Nevertheless, our analysis

350 confirmed that cluster 4 is predominantly composed of TE-like cells, while the remaining clusters retain
351 EPI identity (Figure 6F, Supplementary Figure 5F-G). This analysis confirmed that the blastoids contain
352 *bona fide* TE-like and EPI-like cells. Overall, the formation of blastoids was achieved using 4 lines in
353 3 different laboratories, demonstrating the robustness of the protocols and their potential for wide
354 adoption in the community.

355 Overall, feeder-free naive hESCs, when aggregated, robustly self-assemble into blastoids containing
356 cells with appropriate lineage identities.

Discussion

Expansion of human naive PSCs on a layer of inactivated MEFs has several limitations. Production of MEFs requires the sacrifice of mice, which contrasts with the 3Rs principles for the ethical use of animals in research. MEF production is also time-consuming and expensive, limiting the range of application of human naive PSCs. Indeed, both mESCs and conventional hPSCs became widespread models only once feeder-free conditions were developed[3,13–15].

The use of MEFs brings an additional hurdle, which is the co-culture of non-human cells with hPSCs. The former might appear as contaminants in global analyses of the latter, as suggested by our analyses of several RNA-sequencing datasets revealing widespread expression of fibroblast markers (Supplementary Figure 2C). Furthermore, the two cell populations might affect each other in a non-controllable manner.

Conventional hPSCs can be expanded without feeders on plates coated with recombinant ECM proteins, such as fibronectin and vitronectin[14,15]. Alternatively, solubilized basement membrane matrixes, commercialised as Matrigel or Geltrex, can be used[13]. However, these substrates have been tested for human naive PSC expansion with only limited success. In some cases (i.e. laminin) only short-term expansion could be achieved, while in others (i.e. Matrigel) stable expansion could be achieved only with additional inhibitors in the media[23,24,53].

Importantly, these substrates are expensive and range from 0.5 to 2 Euros/cm^2. In contrast, the cost of using serum coating is reduced by two orders of magnitude to around 0.5 cents/cm^2, while allowing for long-term expansion without requiring any additional changes in media formulation or culture regime.

For all these reasons, serum-coating represents a significant improvement over current methodologies, allowing for the widespread use of naive hPSCs for several applications, such as large-scale screenings, epigenetic and metabolic profiling, and the generation of embryo models such as blastoids. Expansion of naive hPSCs on serum resulted in a streamlined blastoid protocol, which worked in multiple laboratories with multiple cell lines, with an efficiency as high as feeder-based protocols.

A recent study showed that human naive PSC colonies are surrounded by laminins and collagens[52], which are, at least in part, produced by naive hPSCs themselves. However, this autocrine ECM protein production is not sufficient for PSC expansion, as either MEFs or exogenous substrates are needed. Our proteomic analysis of the FBS coating allowing for human naive PSC expansion revealed the presence of several Collagens, Laminins, together with Vitronectin and Fibronectin. We, therefore, speculate that this combination of ECM proteins is crucial for naive hPSC expansion, but future functional studies will be needed to tease out the contribution of each individual ECM protein.

Implementing our approach requires batch testing of serum, a standard procedure for over 40 years, also required for the culture of mESCs with serum-based media[79]. Indeed, in our experience, FBS batches

allowing robust expansion of mouse ESCs all worked well for providing growth substrates for naive hESCs.

We also observed that harsh treatments, such as growth at clonal density after fluorescence-activated cell sorting in the presence of antibiotics are better tolerated on feeders. Thus, some procedures, such as genomic engineering, might be performed preferably on MEFs. Genomic engineering on mESCs via homologous recombination has been performed on feeders for similar reasons[80–84]. We note that shuttling serum-adapted hESCs between serum coating and MEFs works without the need for re-adaptation to feeder-free conditions.

Finally, this manuscript represents a joint effort of several laboratories routinely working with naive hPSCs. Once a methodology was identified by one lab, reagents and protocols were shared with other labs, resulting in extensive testing of multiple lines for different applications before publication. This constructive and cooperative approach allowed us to quickly build trust in our methodology, thanks to the testing performed in parallel by 5 labs.

Materials and Methods

Culture of hPSCs

Naive hiPSCs HPD06 and HPD03 were previously generated by direct reprogramming from somatic cells as described in[30] were cultured on mitotically inactivated mouse embryonic fibroblasts (MEFs; DR4 ATCC), serum coating (10% Fetal Bovine Serum [Gibco A5256701] in DMEM high glucose [Gibco 41965039]) (vol/vol in PBS with $MgCl_2/CaCl_2$, Merck Sigma Aldrich D8662) in PXGL medium [32] at 37°C, 5% CO_2, 5% O_2. The PXGL medium was prepared as follows: N2B27 (DMEM/F12 [Gibco 11320074], and Neurobasal in 1:1 ratio [Gibco 21103049], with 1:200 N2 Supplement [Gibco 17502048], and 1:100 B27 Supplement [Gibco 17504044], 2 mM L-glutamine [Gibco 25030024], 0.1 mM 2-mercaptoethanol [Merck Sigma Aldrich M3148]) supplemented with 1 µM PD0325901 (Axon Medchem 1408), 2 µM XAV939 (Axon Medchem 1527), 2 µM Gö6983 (Axon Medchem 2466) and 10 ng/ml human LIF (Qkine Qk036). Cells were passaged as single cells every 3-4 days at a split ratio of 1:3 or 1:4 following dissociation with TrypLE (Gibco 12563029) for 3 minutes at room temperature. 10 µM ROCK inhibitor (ROCKi, Y27632, Axon Medchem 1683) was added to the naive medium for 24 hours after passaging. For the feeder-free conversion, naive hiPSCs HPD06 and HPD03 stably cultured on MEFs were collected with ReLeSR (STEMCELL Technologies 100-0483). Cells were first incubated for 2 minutes at room temperature, followed by another 5 minutes at 37°C after the complete aspiration of the reagent. Cells were collected by carefully washing the well with fresh PXGL medium adding 10 µM ROCKi and were plated on feeder-free plates coated with serum at a 1:1 to 1:2 ratio.

Naive hESCs H9[1] from Leeb's group and Shef6[85] were cultured on mitotically inactivated DR4 MEFs or serum coating (DMEM high glucose [Sigma-Aldrich D5671] and 10% FBS (Sigma-Aldrich F7524 or Biowest S1600) in PXGL at 37°C, 5% CO_2, 5% O_2. Cells were passaged every 3-4 days at a split ratio up to 1:12 using Accutase (Merck Sigma Aldrich A6964) for 5 minutes at 37°C. 10 µM ROCK inhibitor was added to the naive medium for 24 hours after passaging. Naive H9 hESCs from Zylicz's group were instead passaged at a split ratio up to 1:6 using TrypLE (Gibco 12563029) for 3 minutes at 37°C.

Naive KOLF2.1J[86] and SCTi003-A (STEMCELL Technologies 200-0511) hiPSCs from Rivron's group were cultured on 0.1% gelatin-coated plates including a feeder layer of irradiated MEFs or serum coating (DMEM high glucose and 10% FBS (Gibco A5256701)) in PXGL at 37°C, 5% CO2, 5% O2. Cells were passaged every 3-4 days in a ratio of 1:6 following dissociation with Accutase (Merck Sigma Aldrich A6964) for 5 minutes at 37°C. 10 µM ROCK inhibitor was added for 24 hours after passaging.

Naive H9 hESCs from Pasque's, SIG-1 hiPSCs (Sigma-Aldrich iPSC EPITHELIAL-1-IPSC0028), and HNES1 hESCs[26] were cultured on MEFs or serum coating (10% Fetal Bovine Serum [Gibco 10270] in DMEM high glucose [Gibco 41966029]) in PXGL at hypoxia conditions in 5% O2 and 5% CO2 incubator under humidified conditions at 37°C. Cells were passaged every 3 days at a split ratio up to

441 1:10 by single-cell dissociation with Accutase (Sigma-Aldrich, A6964-100ML) for 5 minutes at 37°C.
442 10 µM ROCK inhibitor was added to the naive medium for 24 hours after passaging.
443 Human primed KiPS[24] were cultured on pre-coated plates with 0.5% growth factor-reduced Matrigel in
444 E8 medium, made in-house according to [15], at 37°C, 5% CO2, 5% O2. Cells were passaged every 3–
445 4 days at a split ratio of 1:8 following dissociation with 0.5 mM EDTA (Invitrogen AM99260G) in PBS
446 without $MgCl_2$/$CaCl_2$ (Merck Sigma Aldrich D8662), pH8.
447 Primed hESCs H9 from Leeb's group (WiCell#WA09) and re-primed Shef6 were maintained feeder-
448 free on plates pre-coated with 1 % (v/v) Geltrex: (Gibco A1413302) in E8 flex (Gibco A2858501)
449 supplemented with 1 % (v/v) Pen/Strep at 37°C, 5% CO2, 5% O2. Following dissociation with Versene
450 (Gibco 15040-033) at room temperature for 5 minutes, cells were passaged every 3-4 days at a split
451 ratio of 1:6.
452 Primed hESCs H9 from Pasque's group were grown in pre-coated geltrex tissue culture at normoxia
453 conditions and under humidified conditions at 37°C in complete E8Flex medium (Thermo Fisher,
454 A2858501). Cells were dissociated into clumps every 5–6 days by incubating 5 min at room temperature
455 in Accutase and passaged at a split ratio of 1:12. 10 µM ROCK inhibitor was added to the naive medium
456 for 24 hours after passaging.
457 All cell lines were routinely checked for mycoplasma and tested negative (Euroclone EMK090020 or
458 Mycoplasma check Service from Eurofins).

459 Capacitation of naive hPSCs

460 Naive hiPSCs HPD06 stably cultured on MEFs or serum coating were capacitated following
461 Rostovskaya *et al*[68] protocol with minor modifications. Briefly, cells were dissociated with TrypLE,
462 and 5×10^4 cells/cm^2 were seeded on a 6-well plate pre-coated with 0.5% growth factor-reduced Matrigel
463 in E8 medium with 10 µM ROCKi (day 0). From day 1 to day 6 cells were cultivated in N2B27 with 2
464 µM XAV939. From day 6 onward the medium was changed to XAF (N2B27 supplemented with 2 µM
465 XAV939, 20 ng/ml Activin A [Qkine Qk001] and 10 ng/ml FGF2 [Qkine Qk002]).
466 Naive hESCs Shef6 and H9 stably cultured on MEFs or serum coating were capacitated following a
467 modified version of the Rostovskaya *et al*[68] protocol. Briefly, cells were dissociated with Accutase and
468 1×10^4 cells/cm^2 or 1.5×10^4 cells/cm^2 were seeded on a 6-well plate pre-coated with Geltrex (Thermo
469 Fisher Scientific A1413302) directly into N2B27 medium supplemented with 10 µM ROCKi (day 0).
470 From day 1, cells were cultivated in N2B27 without ROCKi. For the additional conditions, the N2B27
471 was supplemented with 2 µM XAV939, 12 ng/mL FGF2 (in-house or PeproTech 100-18B) and/or 10
472 ng/mL Activin A (PeproTech 120-14E) or replaced with E8 or mTeSR.

473 ## Conversion of human naive PSCs into trophectoderm/TSCs

474 Naive hiPSCs HPD06 and HPD03 stably cultured on MEFs or serum coating were pre-treated on MEF
475 with TS medium for 24h. Cells were dissociated with TrypLE, and 5×10^4 cells/cm^2 were seeded on a
476 6-well plate pre-coated with 5 µg/mL Collagen IV and further cultured in TS medium (DMEM/F12
477 supplemented with 0.1 mM 2-mercaptoethanol, 0.2% FBS, 0.3%, Bovine serum albumin (BSA, Gibco
478 15260-037), 1% ITS-X (Gibco 51500), 1.5 µg/ml L-ascorbic acid (Merck Sigma Aldrich A4544), 50
479 ng/ml EGF (Qkine Qk011), 2 µM CHIR99021 (Axon Medchem 1386), 0.5 µM A83-01 (Axon
480 Medchem 1421), 1 µM SB431542 (Axon Medchem 1661), 0.8 mM VPA [HDACi, Merck Sigma
481 Aldrich P4543], and 5 µM ROCKi). Cells were cultured in 5% CO_2 and 5% O_2 changing medium every
482 2 days and were passaged upon 80% confluency at a 1:6 to 1:8 ratio.
483 Naive SIG-1 hiPSCs to trophoblast differentiation was done as previously published[39], using the
484 following previously described protocols for hTSCs[34–36,70]. Cells were cultured on MEFs or serum
485 coating until subconfluency and dissociated in single-cell using TryplE for 5 min at 37°C in PXGL
486 supplemented with 10 mM Y-27632 (Tocris, 1254). At day 2 of culture, cells were washed with PBS
487 (Gibco, 10010-015), and the media was switched from PXGL to ASECRiAV medium[87] consisting of
488 DMEM/F12 (Gibco, 31330038) supplemented with 0.3% BSA (Sigma A3059), 0.2% FBS (Gibco
489 10270-106), 1% Penicillin-streptomycin (Gibco 15140-122), 1% insulin-transferrin-selenium-
490 ethanolamine-X 100 supplement (Gibco 51500056), 1.5 mg/mL L-ascorbic acid (Sigma A8960), 0.5
491 mM A83-01 (Peprotech 9094360), 1 mM SB431542 (Axon Medchem 1661), 50 ng/ml hEGF (Miltenyi
492 Biotec 130-097-750), 2uM CHIR99021 (Axon Medchem 1386), 0.8 mM Valproic acid (Sigma
493 V0033000), 0.1 mM b-mercapto-EtOH (Gibco 31350- 010) and 5 mM Y-27632 (Tocris 1254). The
494 medium was changed every day and supplemented with 5 mM Y-27632. From passage 1 onwards
495 hTSCs were cultured and maintained on 1.5 mg/mL iMatrix-silk-E8-Laminin overnight coated tissue
496 culture treated plates in hypoxia conditions 5% O2 and 5% CO2 at 37°C and passaged every 5 days at
497 1:3 splitting ratio. hTSCs used in all experiments were cultured and maintained in ASECRiAV until
498 day 26 of conversion.
499 Naive SIG-1 hiPSCs differentiation to trophectoderm was performed as previously described[88]. Briefly,
500 cells were dissociated in single cells using Accutase at 37°C for 6 min, followed by gentle mechanical
501 dissociation. Single cells were counted and viability was assessed via trypan blue staining using
502 ThermoFisher Countess II and 3×10^4 live cells/cm^2 were plated onto iMatrix Silk laminin 511-coated
503 plate (Amsbio AMS.892 012) in nTE1 media (N2B27 supplemented with 2 µM A83-01 [Merck Sigma
504 Aldrich SML0788], 2 µM PD0325901 [Axon Medchem 1408], 10 ng/ml BMP4 [R&D Systems 314-
505 BP] and 10 µM Y-27632 [Tocris 1254]). After 24h, cells were washed with PBS and media switched
506 to nTE2 for 48h and refreshed daily (N2B27 supplemented with 2 µM A83-01, 2 µM PD0325901 and
507 1 µg/ml JAKi1 [Merck Sigma Aldrich 420099]). Cells were fixed on day 3.

508 ## Culture of BAP-treated primed pluripotent stem cells

509 MEFs were fed with DMEM/Ham's F-12 medium containing 0.1 mM 2-mercaptoethanol, 1% Insulin-
510 Transferrin-Selenium-Ethanolamine (ITS-X; Gibco 51500056), 1% non-essential amino acids (NEAA;
511 Gibco 11140050), 2 mM L-glutamine, and 20% KnockOut™ Serum Replacement (KSR; Gibco
512 10828028) for 24 h. The supernatant was collected and used as MEF-conditioned medium. KiPS were
513 dissociated into single cells with TrypLE. The cells were cultured on pre-coated plates with 0.5%
514 growth factor-reduced Matrigel at a density of 2×10^4 cells/cm^2 with MEF-conditioned medium
515 supplemented with 10 ng/ml BMP4 (Peprotech 120-05ET), 1 μM A83-01, 0.1 μM PD173074 (Axon
516 Medchem 1673), and 10 μM ROCKi, as described previously[36]. The medium was changed daily.

517 ## Spontaneous differentiation with embryoid bodies

518 Capacitated hiPSCs HPD06 from stable cultures on MEFs or serum coating were single-cell dissociated
519 with TrypLE and seeded at 1.5×10^4 cells in v-bottom 96-well plates (Greiner, M9686) pre-treated with
520 anti-adherence AggreWell™ Rinsing Solution (STEMCELL Technologies 7010) in E8 medium with
521 10 μM ROCKi (day 0). From day 1, aggregates were cultivated in spontaneous differentiation medium
522 (DMEM/F12 with 20% FBS, 2 mM L-glutamine, 1% NEAA and 0.1 mM 2-mercaptoethanol). Half of
523 the medium was changed every 2 days.

524 ## Blastoid formation

525 Blastoid experiments from naive H9 hESCs were performed according to Kagawa *et al*[41], with minor
526 modifications. Briefly, H9 naive hESCs were collected by incubation for 3 min with Accutase (Merck
527 Sigma Aldrich A6964). Single cells were plated at a density of 98-102 cells per micro-well of a 24-well
528 AggreWell™400 plate in N2B27 supplemented with 10 μM Y27632 (Axon Medchem 1683) to
529 aggregate for 3h. Subsequently, half medium was changed with 2x PALLY consisting of N2B27
530 supplemented with 1 μM PD0325901 (Axon Medchem 1408), 1 μM A83-01 (Axon Medchem 1421),
531 10 ng/mL hLIF (Qkine Qk036), 1 μM oleoyl-L-α-lysophosphatidic acid sodium salt (LPA, Merck
532 Sigma Aldrich L7260) and Y27632. 24 hours later, half-medium was changed with 1x PALLY. After
533 48h of PALLY culture, blastoids were maintained for 56 hours in LY medium consisting of N2B27
534 supplemented with LPA and Y27632. Blastoids from H9 naive hESCs were processed for single-cell
535 RNA sequencing at day 5.
536 Blastoid experiments from naive KOLF2.1J and SCTi003-A hiPSCs were performed according to
537 Kagawa et al.[41], with minor modifications. Naive KOLF2.1J and SCTi003-A hiPSCs were collected by
538 incubation with Accutase for 5 min. In the presence of MEFs, cells were incubated for 70 minutes on
539 0.1% gelatin-coated plates after which the non-attached hiPSCs were collected. Single cells were plated
540 at a density of 20.000 cells per well of a 96-well plate comprising microwells of 200 μm diameter, made
541 as previously described[89]. Cells were cultured in N2B27 supplemented with 0.3% BSA (Sigma Aldrich

542 A7979), 1μM PD0325901 (MedChem Express HY-10254), 1μM A83-01 (MedChem Express HY-
543 10432), 10ng/ml hLIF (in house), 1 μM LPA (Peprotech 2256236) and 1:1000 CEPT cocktail (Thermo
544 Fisher A56799). After 24 hours the medium was changed to N2B27 supplemented with 1 μM
545 PD0325901, 1 μM A83-01, 10 ng/ml LIF and 1 μM LPA for 48 hours with daily medium changes.
546 Blastoids were maintained for an additional 48 hours in N2B27 medium supplemented with 1 μM LPA.
547 Blastoid experiments from naive HNES1 hESCs were performed as previously described[41] using
548 AggreWells™400 (STEMCELL Technologies 34415). Briefly, naive HNES1 hESCs were treated with
549 Accutase at 37°C for 6 min, followed by gentle mechanical dissociation. Cell pellet was resuspended
550 in aggregation medium composed by N2B27 with 0.3% BSA (Merck Sigma Aldrich A7979) and 10
551 μM Y-27632. Single cells were counted and viability assessed via trypan blue staining using
552 ThermoFisher Countess II and $1.0/1.2\times10^5$ live cells/well (~80/100 cells/μwell) were seeded into
553 AggreWells™400 and grown in a hypoxic chamber. AggreWells™400 were treated with an anti-
554 adherent solution (STEMCELL Technologies 07010) and washed 3 times (2x N2B27 and 1x
555 aggregation medium) before cell plating (day -1). The cells were allowed to form aggregates inside the
556 microwell for 24 h. On day 0, the aggregation medium was replaced with PALLY medium: N2B27
557 with 0.3% BSA, 1 μM PD0325901, 1 μM A83-01 (Merck Sigma Aldrich SML0788), 0.5 μM LPA
558 (Tocris 3854), 10 ng/ml hLIF and 10 μM Y-27632. PALLY medium was refreshed on day 1. After 48
559 h (day 2) PALLY medium was replaced with N2B27 containing 0.3% BSA, 0.5 μM LPA and 10 μM
560 Y-27632 (LY medium). LY medium was refreshed on day 3, and blastoids fully formed on day 4.

561 Proliferation assay and AP staining

562 Cell proliferation was assessed by plating 5×10^4 cells/cm^2 in a 6-well plate. Cells were single-cell
563 dissociated with TrypLE, counted and re-plated every 3 days.
564 For AP staining, cells were fixed with a citrate–acetone–formaldehyde solution and stained using the
565 Alkaline Phosphatase kit (Merck Sigma Aldrich 86R-1KT). Plates were scanned using a Nikon Scanner
566 and scored with the Analyse Particles plugin of ImageJ (pixels 5-500, circularity 0.5-1).

567 Gene expression analysis by quantitative PCR with reverse transcription

568 Total RNA from naive hiPSCs HPD06 and HPD03 was isolated using Total RNA Purification Kit
569 (Norgen Biotek 37500), and complementary DNA (cDNA) was made from 500 ng using M-MLV
570 Reverse Transcriptase (Invitrogen 28025-013) and dN6 primers. Data were acquired with
571 QuantStudio™ 6&7 Flex Software 1.0.
572 Total RNA from naive hESCs H9 and Shef6 was isolated with the ExtractMe kit (Blirt EM15) following
573 the manufacturer's instructions, and cDNA was made from 100 ng using the SensiFAST cDNA
574 Synthesis Kit (Bioline BIO-65054). Real-time PCR was performed on the CFX384 Touch real-time
575 PCR detection system (Bio-Rad).

576 SYBR Green Master mix (Bioline BIO-94020) was used for real-time qPCR and primers are listed in
577 Supplementary Table 1. *β-ACTIN* or *GAPDH* were used as endogenous controls to normalise
578 expression. Three technical replicates were carried out for all RT-qPCR.

579 Immunofluorescence

580 Immunofluorescence analysis of naive hiPSCs HPD06 and HPD03 was performed on 1% Matrigel-
581 coated glass coverslip in wells. Cells were fixed in 4% Formaldehyde (Merck Sigma Aldrich 78775) in
582 PBS for 10 min at room temperature, washed in PBS, and permeabilised and blocked in PBS with 0.3%
583 Triton X-100 (PBST) and 5% of horse serum (ThermoFisher 16050-122) for 1 hour at room
584 temperature. Cells were incubated overnight at 4°C with primary antibodies in PBST with 3% horse
585 serum. After washing with PBS, cells were incubated with secondary antibodies (Alexa, Life
586 Technologies) for 45 min at room temperature. Nuclei were stained using Fluoroshield™ with DAPI
587 (Merck Sigma Aldrich F6057). Images were acquired with a Zeiss LSN700 confocal microscope using
588 ZEN 2012 software. Fluorescence intensity was quantified using Cell Profiler software (v4.2.1). DAPI
589 staining was used to identify individual nuclei of cells. 5 independent fields from 3 replicates were
590 quantified for each sample, for a total of 500 cells per sample. Single-cell measured mean intensity
591 values were considered for downstream data analysis.
592 For immunofluorescence analysis of naive hESCs H9 from Leeb's group and Shef6, cells were plated
593 onto μ-Slide 8 Well Glass Bottom Chamber Slides (Ibidi 80827) with MEFs, or onto slides coated with
594 serum or Geltrex. Cells were fixed in 4% Formaldehyde in PBS for 20 min at room temperature, washed
595 in PBS, and permeabilized and blocked in PBS with 0.5 % Triton X-100 (PBST) and 5% BSA for 30
596 min at room temperature. Cells were incubated overnight at 4°C with primary antibodies in PBST with
597 5% BSA. After washing with PBS, cells were incubated with secondary antibodies (Alexa, Life
598 Technologies) for 1h at room temperature. After washing with PBS, the nuclei were stained with 20
599 ng/mL DAPI in PBS (Invitrogen D1306) for 5 min in the dark at room temperature. Samples were
600 mounted using Vectashield with DAPI (Vector Laboratories VECH-1200). Images were acquired with
601 an Axio Observer Z1 microscope.
602 Immunofluorescence staining protocol was performed in naive H9 hESCs from Pasque's group and
603 SIG-1 hiPSC as previously published[39,90]. Cells were grown on 0.1% gelatinized 18 mm round
604 coverslips on MEFs or serum coating. Cells were fixed in 4% paraformaldehyde-PBS for 10 min at
605 room temperature in the dark and permeabilized with 0.5% Triton X-100 in PBS for 5 min and washed
606 twice with 0.2% Tween 20 in PBS (PBST) for 5 min each before proceeding to the staining. Primary
607 and secondary antibodies were diluted in a blocking buffer containing mainly 2% Tween-PBS with 5%
608 normal donkey serum and 0.2% fish skin gelatin. Cells on coverslips were incubated overnight at 4°C
609 with the specific primary antibodies in blocking solutions (1:50 dilution for NANOG, 1:300 dilution
610 for KLF17), then washed three times with PBST for 5 min. After washing, the samples were incubated

611 with secondary antibodies diluted in blocking buffer for 1 hour in the dark at room temperature. The
612 samples were then washed with PBST three times for 5 min each and afterwards washed with 0.002%
613 DAPI (Sigma-Aldrich D9542) solution in PBST. The coverslips were mounted in Prolong Gold reagent
614 with DAPI after a final wash in PBST. Naive hPSCs immunofluorescence images were taken in a Nikon
615 TiE A1R inverted microscope and processed in ImageJ. Brightfield images were taken using a Nikon
616 Eclipse Ti2 microscope and analyzed using ImageJ software.
617 Blastoids from naive H9 hESCs were fixed with 4% paraformaldehyde for 20 min at room temperature.
618 Subsequently, the samples were washed for 3 times 10 minutes with PBST (PBS containing 0.1%
619 Tween20) supplemented with BSA (0.3%). The samples were then permeabilised for 20 min using 0.2%
620 Triton X-100 in PBS and afterwards blocked using a blocking buffer containing 0.1% Tween20, 1%
621 BSA and 10% normal donkey serum in PBS for at least 3 hours. The samples were then incubated
622 overnight at 4°C with primary antibodies diluted in blocking buffer. The next day, samples were washed
623 with PBST at least three times for 10 min each. After washing, the samples were incubated with
624 secondary antibodies diluted in blocking buffer for 3 hours in the dark at room temperature. The samples
625 were then washed with PBST three times for 10 min each and afterwards mounted using PBS. Image
626 acquisition was performed using a Leica Stellaris 5 fluorescence confocal microscope.
627 Blastoids from naive KOLF2.1J and SCTi003-A hiPSCs were fixed with 4% PFA for 30 min at room
628 temperature and rinsed three times with PBS. Samples were permeabilized and blocked using 0.3%
629 Triton X-100 and 10% normal donkey serum in PBS for at least 60 min and incubated overnight at
630 room temperature with primary antibodies diluted in fresh blocking/permeabilization buffer. The
631 following day samples were washed with PBS containing 0.1% Triton X-100 (PBST) at least three
632 times for 10 min each. Samples were then incubated in Alexa Fluor-tagged secondary antibodies
633 (Abcam or Thermofisher Scientific) diluted in PBST for at least 30 min in the dark at room temperature
634 and washed three times with PBST for 10 min each.
635 Blastoids from naive HNES1 hESCs were fixed with 4% PFA for 30 min at room temperature and
636 rinsed three times with PBS. About 10-20 structures per condition were then moved to Thermo
637 Scientific™ Nunc™ MiniTrays with Nunclon™ Delta surface and permeabilised for 30 min at RT using
638 PBS/0.3% Triton X-100 (Merck Sigma Aldrich). Cells were blocked for 4-6h at RT with blocking
639 solution (PBS 0.3% Triton X-100 with 10% Normal Donkey Serum [Merck Sigma Aldrich S30]).
640 Primary antibodies (listed in Supplementary Table 2) were diluted in blocking solution and incubated
641 overnight at 4°C in a humidified chamber. Cells were washed three times with PBS 0.1% Triton X-100,
642 and stained with secondary antibodies for 1h at RT in a humidified chamber. Cells were washed three
643 times with PBS 0.1% Triton X-100, and stained with DAPI for 15 min at RT during the second wash
644 (0.1 µg/ml DAPI in PBS 0.1% Triton X-100). Finally, blastoids were moved into IBIDI µ-Slide 15 Well
645 3D Glass Bottom (81507) and imaged using a C2 or TiE A1R confocal microscopes (Nikon). Images
646 were processed using the software Fiji (ImageJ), Z-stacks were shown as Max Intensity projections and

647 denoised using the "despeckle" tool equally on all images. Brightfields were taken using an EVOS
648 M3000 microscope.
649 All used primary antibodies are listed in Supplementary Table 2.

650 Flow cytometry

651 For flow cytometry analysis, naive and differentiating Shef6 hESCs and primed hPSCs were detached
652 using Accutase and resuspended in DMEM supplemented with 0.5% BSA. For surface marker staining
653 the cells were washed 1x in FACS buffer (1x PBS and 1% BSA), stained with APC-conjugated anti-
654 human SUSD2 antibody (BioLegend 327408) diluted 1:100 in FACS buffer for 30 min on ice in the
655 dark and washed again 1x with FACS buffer. For live/dead discrimination 5 µg/mL DAPI (Invitrogen
656 D1306) was used. Antibody signal levels were measured using the LSR Fortessa (BD Bioscience) or
657 ZE5 (Bio-Rad) and then analysed with the FlowJo software (v10, BD Bioscience).
658 Nave H9 hESCs and SIG-1 hiPSCs were first stained for viability in 1:300 Live/Death Zombie Aqua in
659 PBS. Fluorophore conjugated antibody was diluted at a ratio of 1:50 in fluorescence-activated cell
660 sorting (FACS) buffer with PE-conjugated anti-human SUSD2 (Biolegend, 327406), for 20 minutes at
661 room temperature, then washed with FACS buffer, and fixed in 4% paraformaldehyde. Cells were
662 passed through a 40 µm cell strainer (Corning 352340). The fluorescence intensity of 20,000 cells was
663 recorded on a flow cytometer (Fortessa X-20 BD Biosciences) and analyzed using FlowJo software.
664 Single-stained controls were used for compensation and gating in the flow cytometer. Only lived cells
665 were used for data analysis.

666 Proteomics

667 Samples were processed using the PreOmics iST sample preparation kit (PreOmics P.O.00027). LC-
668 MS/MS analysis consisted of a NanoLC 1200 coupled via a nano-electrospray ionization source to the
669 quadrupole-based Q Exactive HF benchtop mass spectrometer [91]. For the chromatographic separation,
670 a binary buffer system consisting of solution A: 0.1% formic acid and B: 80% acetonitrile, 0.1% formic
671 acid was used. Peptides were separated according to their hydrophobicity on an analytical column (75
672 µm) in-house packed with C18-AQ 1.9 µm C18 resin with a gradient of 7–32% solvent B in 45 min,
673 32–45% B in 5 min, 45–95% B in 3 min, 95–5% B in 5 min at a flow rate of 300 nl/min. MS data
674 acquisition was performed in DIA (Data Independent Acquisition) mode using 32 variable windows
675 covering a mass range of 300–1650 m/z. The resolution was set to 60'000 for MS1 and 30'000 for MS2.
676 The AGC was 3e6 in both MS1 and MS2, with a maximum injection time of 60 ms in MS1 and 54 ms
677 in MS2. NCE was set to 25%, 27.5%, 30%. All acquired raw files were processed using Spectronaut
678 software (17.0). For protein assignment, spectra were correlated with the Rattus Norvegicus/Bos Taurus
679 database (v. 2023). Searches were performed with tryptic specifications and default settings for mass
680 tolerances for both MS and MS/MS spectra.

681 The other parameters were set as follows. Fixed modifications: Carbamidomethyl (C); variable
682 modifications: Oxidation, Acetyl (N-term); digestion: Trypsin, Lys-C; min. peptide length = 7Da; max.
683 peptide mass = 470Da; false discovery rate for proteins and peptide-spectrum = 1%. Perseus software
684 (1.6.2.3) was used to logarithmise, group and filter the protein abundance. The obtained list of proteins
685 was analysed using the Matrisome AnalyseR tool
686 (https://sites.google.com/uic.edu/matrisome/tools/matrisome-analyzer[62]) from The Matrisome Project.

687 Exome sequencing

688 NEGEDIA S.r.l. performed the Exome Sequencing service. Genomic DNA was extracted with a
689 paramagnetic beads technology using the Negedia DNA extraction service, quantified using the Qubit
690 4.0 fluorimetric Assay (Thermo Fisher Scientific) and sample integrity, based on the DIN (DNA
691 integrity number), was assessed using a Genomic DNA ScreenTape assay on TapeStation 4200 (Agilent
692 Technologies). Libraries were prepared from 100 ng of total DNA using the NEGEDIA Exome
693 sequencing service which included library preparation, target enrichment using Agilent V8 probe set,
694 quality assessment with FastQC v0.11.9 (https://www.bioinformatics.babraham.ac.uk/projects/fastqc/)
695 and sequencing on a NovaSeq 6000 system using a paired-end, 2x150 cycle strategy (Illumina Inc.).
696 The raw data were analysed by NEGEDIA Exome pipeline (v1.0) which involves, alignment to the
697 reference genome (hg38, GCA_000001405.15), removal of duplicate reads and variant calling with
698 Sentieon 202308[92]. Variants were annotated by the Ensembl Variant Effect Predictor (VEP) tool3 (v.
699 104)[93]. Annotated variants were selected based on: impact on protein
700 High/Moderate, base depth ≧30, alternate depth ≧5 and alt/base depth ≧5%.
701 Selected variants were finally classified with Varsome Clinical
702 (https://eu.clinical.varsome.com/).

703 Bulk RNA sequencing and analysis

704 Total RNA from HPD06 and HPD03 naive hiPSCs was isolated as previously described, and Quant
705 Seq 3' mRNA-seq Library Prep kit (Lexogen) was used for library construction. Before sequencing
706 library quantification was performed by fluorometer (Qubit) and bioanalyzer (Agilent). Sequencing is
707 performed on NextSeq500 ILLUMINA instruments to produce 5 million reads (75bp SE) for each
708 sample. Transcript quantification was performed from raw reads using Salmon (v1.6.0)[94] on transcripts
709 defined in Ensembl 106. Gene expression levels were estimated with tximport R package (v1.26.1)[95].
710 Batch correction was performed using ComBat_seq function from the sva R package (v3.50.0;
711 https://bioconductor.org/packages/release/bioc/html/sva.html). Batches have been defined following
712 library preparation: batch 1 for full-length libraries and batch 2 for Quant Seq 3′ mRNA-seq Library
713 Prep kit. CPM on batch corrected counts were computed using the cpm function of the edgeR package
714 (v4.0.12[96]). PCA was performed using the svd r function on log-transformed CPM. All plots except the

715 heatmaps have been done using ggplot2 v3.5.1 (https://ggplot2.tidyverse.org/authors.html#citation).
716 Heatmap was done using pheatmap R package (v1.0.12). All analyses were performed using R v4.3.2.
717 Imprinted genes analysis of HPD00 primed and HPD06 and HPD03 naive hiPSCs have been performed
718 by submitting the .fastq raw files to BrewerIX (https://brewerix.bio.unipd.it)[45], implementing the
719 complete pipeline and evaluating the significant genes.
720 Total RNA from naive hESCs Shef6 was isolated as previously described. Library preparation with the
721 Quant Seq 3' mRNA-seq Library Prep kit (Lexogen) and sequencing with the Illumina NextSeq2000
722 P3 platform was carried out at the VBCF NGS facility, producing 5-10 million reads (50 bp SE). For
723 analysis of the fastq files the Nextflow 23.04.1.5866/nf-core/rnaseq v3.10.1 pipeline was used. This
724 included quality control with fastQC (v0.11.9), pseudo-alignment to the human reference genome hg38
725 with Salmon (v1.9.0) and alignment with STAR (v2.7.10a). Gene expression levels were estimated with
726 the tximport R package (v1.26.1)[95]. DESeq2 (v1.38.3) was used for further analysis including
727 differential expression analyses. For comparison with already published data[68], batch correction was
728 performed using ComBat_seq function from the sva R package (v3.46.0). For PCAs, counts were
729 transformed with the regularised log transformation (rlog) function (for own time course) or the
730 variance-stabilising transformation (vst) function (integration with Rostovskaya data) from DESeq2.
731 All plots except heatmap have been done using ggplot2 v3.5.1. Heatmaps were done with the pheatmap
732 R package (v1.0.12) using row-wise z-transformed DESeq2-normalized counts. All analyses were
733 performed using R v4.3.2.

734 Single-cell RNA sequencing, analysis and comparison with bulk RNA 735 sequencing

736 For the analyses of the pluripotency exit, the human embryogenesis reference dataset[69] was derived by
737 the integration of six published human datasets[20,40,75–78] covering developmental stages from the zygote
738 to the gastrula was kindly provided by the Petropoulos lab. Analysis was performed using Seurat v5.1.0
739 and the data was subset for embryonic cells covering E5-E14. For the PCA, pseudobulk data was
740 generated with Seurat's AggregateExpression function and integrated with the bulk RNA-seq data using
741 DESeq2 v1.38.3. Batch correction for the datasets was performed using the ComBat_seq function
742 before applying variance stabilising transformation with the vst function from DESeq2. Heatmaps and
743 boxplots were generated using the Shiny app (http://petropoulos-lanner-labs.clintec.ki.se) from the
744 reference dataset[69].
745 For blastoids validation blastoids were dissociated into a single cell suspension by incubation with a
746 mixture of TrypLE™ (Thermo Fisher Scientific A1217701) and Accutase (Merck Sigma Aldrich
747 A6964). The sample was incubated with 0.5 µg of unique hashtag antibody for 20 min on ice. TotalSeq
748 hashtag antibodies (Biolegend) were used to multiplex the samples[97]. The sample was sorted on a BD
749 FACSymphony S6 (BD Bioscences) and then loaded onto a Chromium Next GEM chip (10x

750 Genomics). Further steps of library preparation were performed according to the Chromium Next GEM
751 Single Cell 3' v3.1 user guide with the addition of the hashtag library for demultiplexing. Combined
752 libraries were sequenced using the NextSeq2000 P2-100 kit (Illumina) with Paired-end sequencing.
753 Initial processing of scRNA-seq data was performed using Cell Ranger (v 6.1.2, 10X Genomics). Dual-
754 indexed RNA and single-indexed hashtag oligo (HTO) libraries were processed in separate instances of
755 cellranger mkfastq, using Illumina's bcl2fastq (v2.20.0.422). FASTQ files were aligned to the human
756 reference genome (GRCh38, v 2020-A as provided by 10x Genomics) with cellranger multi (expect-
757 cells 16500, min-assignment-confidence 0.9), assigning 4251 cells to the sample of interest. The
758 resulting filtered feature-barcode matrix was loaded into Seurat (v 4.3.0)[98], excluding features that were
759 detected in less than three cells. Next, RNA data was normalized with default LogNormalize method,
760 and HTO assay was normalized with centered log-ratio (CLR) transformation. Based on QC plots, cells
761 with more than 15% mitochondrial counts or less than 7000 UMIs (nCount_RNA) were removed,
762 retaining 3260 high-quality cells. These were subjected to standard Seurat processing using mostly
763 default parameters unless indicated: FindVariableFeatures, ScaleData, RunPCA, RunUMAP
764 (dims=1:15), FindNeighbors (dims=1:15), FindClusters (resolution=0.5). To characterize the cells'
765 cycling status, the function CellCycleScoring was run using the built-in lists of S and G2M phase
766 markers (cc.genes.updated.2019) derived from[99]. Cells separated by cell cycle phase on the UMAP and
767 this source of heterogeneity was then regressed out using ScaleData (vars.to.regress = c("S.Score",
768 "G2M.Score"), features = rownames(object)), followed by RunPCA, RunUMAP(dims=1:15),
769 FindNeighbors(dims=1:15), and FindClusters(resolution=0.5), resulting in 5 clusters. The raw counts
770 of the quality-filtered matrix was uploaded to the Early Embryogenesis Projection Tool (v2.1.1)
771 (https://petropoulos-lanner-labs.clintec.ki.se/shinys/app/ShinyEmbryoProjP, accessed on 2024-09-26)
772 to project the cells on an integrated reference UMAP of human embryo development and get annotation
773 of predicted cell identities[69].

774 Statistics and reproducibility

775 For each dataset, sample size *n* refers to the number of biological or technical replicates, shown as dots
776 and stated in the figure legends. All error bars indicate the standard error of the mean (SEM). All RT-
777 qPCR experiments were performed in three technical replicates.

778 Ethics statement

779 Our research complies with all relevant ethical regulations including ISSCR guidelines.
780 HPD06 and HPD03 naive hiPSCs used in G.M.'s Laboratory were checked by the European ethics
781 committee and registered in the human pluripotent stem cells registry (link: https://hpscreg.eu/ cell-
782 line/UNIPDi004-B). Experiments with hPSCs and blastoids in J.J.Z's Laboratory were approved by
783 the Scientific Ethics Committee for Hovedstaden (H-21043866/94634 and H-24048289). Shef6 line use

is with the agreement of the Steering Committee of the UK Stem Cell Bank (SCSC16-09). The WiCell line H9 (WA09) was used under the agreements 23-W0460 (JJZ) and 21-W0002 (ML). Work with human embryonic and induced pluripotent stem cells including blastoids in V.P. Laboratory was approved by the UZ/KU Leuven ethics committee (S64962, S66595 and S68981). Work with mouse embryonic fibroblast was approved by the UZ/KU Leuven ethics committee (P170/2019). The Austrian Academy of Sciences (the local ethical body) has given N.R.'s Laboratory a license to perform blastoid experiments, following expert legal advice that concluded these are not in conflict with Austrian laws. This license is in the shape of a statement of the Commission for Science Ethics of the Austrian Academy of Sciences concerning the project 'Modeling human early development using stem cells'. There is no approval number on that document. This license conforms with the ethical standards suggested by the International Society for Stem Cell Research (ISSCR). This work did not exceed a developmental stage normally associated with 14 consecutive days in culture after fertilization nor did it entail any implantation *in vivo*.

Data availability

Bulk and single-cell RNA-seq data for this study have been deposited in the Gene Expression Omnibus (GEO) database under the accession code GSE284370. We also included available RNA-Seq data for naive and primed hPSCs, hTSCs and fibroblasts from GSE110377[30], GSE63577[100], GSE93226[101], GSE75868[43], GSE184562[72], GSE138688[34], GSE178162[102], GSE135695[103], PRJNA397941[27], GSE133630[104], GSE73211[105], PRJEB7132[24], PRJEB12748[26]; for capacitation from GSE123055[68]; for embryonic development from the human embryogenesis reference dataset[69], comprehensive of GSE36552[20], E-MTAB-3929[75], GSE136447[76], E-MTAB-9388[78], GSE171820[40], PRJEB30442[77]. Proteomics data have been deposited in the PRIDE Proteomics database under the accession code PXD059820.

Acknowledgements

We thank the KU Leuven FACS Core team for supporting flow cytometry experiments, Alejandra Purcell from Gorgas Institute in FACS analysis, and the VIB BioImaging Core Leuven for their contribution to imaging performed in V.P. lab. We thank the Vienna Biocenter Core Facilities (VBCF) for support in NGS analysis. J.J.Z's team thanks Antar Drews and Sandra Bages Arnal for their input, the reNEW platforms for technical expertise, support and use of equipment in particular: H. Wollmann, M. Michaut, J. Bulkescher, G. Dela Cruz and A. Kalvisa.

G.M.'s Laboratory is supported by grants from: Giovanni Armenise–Harvard Foundation, Telethon Foundation (GJC21157), European Research Council Starting Grant (716910 - MetEpiStem), Italian national project 'PRIN 2022' (2022RA8E3T) and La Caixa Foundation (LCF/PR/HR24/52440015). G.R. is supported by a HORIZON MSCA Postdoctoral Fellowship (101108873 - PLURImet). M.L.'s Laboratory is supported by grants from the Austrian Science Fund (FWF; P35637, I5958). M.O. is a member of the FWF-funded doctoral programme 'Signalling Molecules in Cellular Homeostasis' (SMICH; W1261), and M.L. is a faculty member and speaker of SMICH and a 'Wiener Wissenschafts-Forschungs- und Technologiefonds (WWTF)' Vienna Research Group Leader (VRG14-006). V.P.'s Laboratory is supported by the Research Foundation-Flanders (FWO grants G0C9320N and G0B4420N to V.P.), KU Leuven Research Fund (C1 grant C14/21/119 to V.P.), and Pandarome project 40007487 (G0I7822N) (funded by the FWO and F.R.S.-FNRS) under the Excellence of Science (EOS) program. M.A.S. is supported by Gorgas Memorial Institute for Health Studies and Fundación Sus Buenos Vecinos in Panama. S.S.F.A.v.K. (11I1523N) and T.X.A.P. (11N3122N) are supported by FWO PhD fellowships. J.J.Z.'s Laboratory is supported by grants from: Novo Nordisk Fonden (NNF21CC0073729), Lundbeckfonden (R345-2020-14979), Danmarks Frie Forskningsfond (0169-00031B) and the European Research Council Starting Grant (101077271 - ChroMeta). N.R.'s Laboratory is supported by the European Research Council (ERC) under the European Union's Horizon 2020 research and innovation programme (ERC-Co grant agreement no. 101002317, "BLASTOID: a discovery platform for early human embryogenesis").

D.C. is supported by Fondazione Telethon Core Grant, Italian Ministry of Health (Piano Operativo Salute Traiettoria 3, T3-AN-09, "Genomed"; Ricerca Finalizzata 2021, "genOMICA"; MCNT2 2023, "EUCARDIS"), Italian Ministry of University and Research and European Union (Next Generation EU - MUR-PRIN-2022, Project PNC 0000001 D3 4 Health). P.G. is supported by Fondazione Telethon Core Grant, AIRC (MFAG 2020), PNRR (PNRR-MR1-2022-12376821), PRIN-2022-PNRR (P2022JLNZ7), PRIN (20224FL9T5). P.M. is supported by Italian national project 'PRIN 2022' (2022LJZRBY)

Author contributions

G.R. performed experiments and analysed data (characterisation, embryonic and TSCs differentiation, bulk RNA-Seq, proteomics), supervised the study, prepared figures and wrote the manuscript; I.Z., performed experiments (characterization) and edited the manuscript; A.D. performed experiments (characterization); G.P. and N.M. performed experiments (characterisation, embryonic and TSC differentiation); P.M. analysed bulk RNA-Seq for the comparison with published datasets; C.C. and D.C. generated and analysed Exome-Seq data; P.G. performed proteomics experiments; G.M. conceived and supervised the study, secured funding and wrote the manuscript. M.O. performed experiments and analysed NGS data (embryonic differentiation), wrote the manuscript and prepared figures; M.L. supervised the study, secured funding and wrote the manuscript. A.O. and E.v.G. performed experiments (blastoids); M.A.S., S.S.F.A.v.K., T.X.A.P., and S.K. performed experiments (characterisation, TSC differentiation); N.R. and V.P. supervised the study, edited the manuscript and secured funding. I.S.B. performed experiments (blastoids), analysed the data, prepared figures and edited the manuscript; A.W. analysed and curated scRNAseq data; J.J.Z. supervised the study, secured funding, prepared figures and wrote the manuscript.

Disclosure and competing interests statement

Davide Cacchiarelli is founder, shareholder, and consultant of NEGEDIA S.r.l. Chiara Colantuono is an employee of NEGEDIA S.r.l.

References

1. Thomson, J. A. *et al.* Embryonic Stem Cell Lines Derived from Human Blastocysts. *Science* **282**, 1145–1147 (1998).
2. Evans, M. J. & Kaufman, M. H. Establishment in culture of pluripotential cells from mouse embryos. *Nature* **292**, 154–156 (1981).
3. Smith, A. G. *et al.* Inhibition of pluripotential embryonic stem cell differentiation by purified polypeptides. *Nature* **336**, 688–690 (1988).
4. Williams, R. L. *et al.* Myeloid leukaemia inhibitory factor maintains the developmental potential of embryonic stem cells. *Nature* **336**, 684–687 (1988).
5. Ying, Q.-L. *et al.* The ground state of embryonic stem cell self-renewal. *Nature* **453**, 519–523 (2008).
6. Martello, G. & Smith, A. The Nature of Embryonic Stem Cells. *Annu. Rev. Cell Dev. Biol.* **30**, 647–675 (2014).
7. Dunn, S.-J., Martello, G., Yordanov, B., Emmott, S. & Smith, A. G. Defining an essential transcription factor program for naïve pluripotency. *Science* **344**, 1156–1160 (2014).
8. Carbognin, E., Betto, R. M., Soriano, M. E., Smith, A. G. & Martello, G. Stat3 promotes mitochondrial transcription and oxidative respiration during maintenance and induction of naive pluripotency. *EMBO J.* **35**, 618–634 (2016).
9. Betto, R. M. *et al.* Metabolic control of DNA methylation in naive pluripotent cells. *Nat. Genet.* **53**, 215–229 (2021).
10. Takahashi, K. *et al.* Induction of Pluripotent Stem Cells from Adult Human Fibroblasts by Defined Factors. *Cell* **131**, 861–872 (2007).
11. Yu, J. *et al.* Induced Pluripotent Stem Cell Lines Derived from Human Somatic Cells. *Science* **318**, 1917–1920 (2007).
12. Hanna, J. *et al.* Human embryonic stem cells with biological and epigenetic characteristics similar to those of mouse ESCs. *Proc. Natl. Acad. Sci.* **107**, 9222–9227 (2010).
13. Ludwig, T. E. *et al.* Feeder-independent culture of human embryonic stem cells. *Nat. Methods* **3**, 637–646 (2006).
14. Braam, S. R. *et al.* Recombinant Vitronectin Is a Functionally Defined Substrate That Supports Human Embryonic Stem Cell Self-Renewal via αVβ5 Integrin. *Stem Cells* **26**, 2257–2265 (2008).
15. Chen, G. *et al.* Chemically defined conditions for human iPSC derivation and culture. *Nat. Methods* **8**, 424–429 (2011).
16. Brons, I. G. M. *et al.* Derivation of pluripotent epiblast stem cells from mammalian embryos. *Nature* **448**, 191–195 (2007).
17. Tesar, P. J. *et al.* New cell lines from mouse epiblast share defining features with human embryonic stem cells. *Nature* **448**, 196–199 (2007).
18. Huang, Y., Osorno, R., Tsakiridis, A. & Wilson, V. In Vivo Differentiation Potential of Epiblast Stem Cells Revealed by Chimeric Embryo Formation. *Cell Rep.* **2**, 1571–1578 (2012).
19. Nichols, J. & Smith, A. Naive and Primed Pluripotent States. *Cell Stem Cell* **4**, 487–492 (2009).
20. Yan, L. *et al.* Single-cell RNA-Seq profiling of human preimplantation embryos and embryonic stem cells. *Nat. Struct. Mol. Biol.* **20**, 1131–1139 (2013).
21. Buecker, C. *et al.* A murine-ES like state facilitates transgenesis and homologous recombination in human pluripotent stem cells. *Cell Stem Cell* **6**, 535 (2010).
22. Chan, Y.-S. *et al.* Induction of a Human Pluripotent State with Distinct Regulatory Circuitry that Resembles Preimplantation Epiblast. *Cell Stem Cell* **13**, 663–675 (2013).
23. Gafni, O. *et al.* Derivation of novel human ground state naive pluripotent stem cells. *Nature* **504**, 282–286 (2013).
24. Takashima, Y. *et al.* Resetting Transcription Factor Control Circuitry toward Ground-State Pluripotency in Human. *Cell* **158**, 1254–1269 (2014).
25. Theunissen, T. W. *et al.* Systematic Identification of Culture Conditions for Induction and Maintenance of Naive Human Pluripotency. *Cell Stem Cell* **15**, 471–487 (2014).
26. Guo, G. *et al.* Naive Pluripotent Stem Cells Derived Directly from Isolated Cells of the Human

Inner Cell Mass. *Stem Cell Rep.* **6**, 437–446 (2016).
27. Liu, X. *et al.* Comprehensive characterization of distinct states of human naive pluripotency generated by reprogramming. *Nat. Methods* **14**, 1055–1062 (2017).
28. Kilens, S. *et al.* Parallel derivation of isogenic human primed and naive induced pluripotent stem cells. *Nat. Commun.* **9**, 360 (2018).
29. Wang, Y. *et al.* Unique molecular events during reprogramming of human somatic cells to induced pluripotent stem cells (iPSCs) at naïve state. *eLife* **7**, e29518 (2018).
30. Giulitti, S. *et al.* Direct generation of human naive induced pluripotent stem cells from somatic cells in microfluidics. *Nat. Cell Biol.* **21**, 275–286 (2019).
31. Dutta, D. *et al.* Self-Renewal Versus Lineage Commitment of Embryonic Stem Cells: Protein Kinase C Signaling Shifts the Balance. *Stem Cells* **29**, 618–628 (2011).
32. Bredenkamp, N. *et al.* Wnt Inhibition Facilitates RNA-Mediated Reprogramming of Human Somatic Cells to Naive Pluripotency. *Stem Cell Rep.* **13**, 1083–1098 (2019).
33. Castel, G. *et al.* Induction of Human Trophoblast Stem Cells from Somatic Cells and Pluripotent Stem Cells. *Cell Rep.* **33**, 108419 (2020).
34. Dong, C. *et al.* Derivation of trophoblast stem cells from naïve human pluripotent stem cells. *eLife* **9**, e52504 (2020).
35. Guo, G. *et al.* Human naive epiblast cells possess unrestricted lineage potential. *Cell Stem Cell* **28**, 1040-1056.e6 (2021).
36. Io, S. *et al.* Capturing human trophoblast development with naive pluripotent stem cells in vitro. *Cell Stem Cell* **28**, 1023-1039.e13 (2021).
37. Linneberg-Agerholm, M. *et al.* Naïve human pluripotent stem cells respond to Wnt, Nodal and LIF signalling to produce expandable naïve extra-embryonic endoderm. *Development* **146**, dev180620 (2019).
38. Okubo, T. *et al.* Hypoblast from human pluripotent stem cells regulates epiblast development. *Nature* **626**, 357–366 (2024).
39. Pham, T. X. A. *et al.* Modeling human extraembryonic mesoderm cells using naive pluripotent stem cells. *Cell Stem Cell* **29**, 1346-1365.e10 (2022).
40. Yanagida, A. *et al.* Naive stem cell blastocyst model captures human embryo lineage segregation. *Cell Stem Cell* **28**, 1016-1022.e4 (2021).
41. Kagawa, H. *et al.* Human blastoids model blastocyst development and implantation. *Nature* **601**, 600–605 (2022).
42. Yu, L. *et al.* Blastocyst-like structures generated from human pluripotent stem cells. *Nature* **591**, 620–626 (2021).
43. Theunissen, T. W. *et al.* Molecular Criteria for Defining the Naive Human Pluripotent State. *Cell Stem Cell* **19**, 502–515 (2016).
44. Pastor, W. A. *et al.* Naïve human pluripotent cells feature a methylation landscape devoid of blastocyst or germline memory. *Cell Stem Cell* **18**, 323–329 (2016).
45. Martini, P. *et al.* BrewerIX enables allelic expression analysis of imprinted and X-linked genes from bulk and single-cell transcriptomes. *Commun. Biol.* **5**, 1–12 (2022).
46. Zhou, W. *et al.* HIF1α induced switch from bivalent to exclusively glycolytic metabolism during ESC-to-EpiSC/hESC transition. *EMBO J.* **31**, 2103–2116 (2012).
47. Gu, W. *et al.* Glycolytic Metabolism Plays a Functional Role in Regulating Human Pluripotent Stem Cell State. *Cell Stem Cell* **19**, 476–490 (2016).
48. Xie, C., Lin, G., Luo, K., Luo, S. & Lu, G. Newly expressed proteins of mouse embryonic fibroblasts irradiated to be inactive. *Biochem. Biophys. Res. Commun.* **315**, 581–588 (2004).
49. Schnabel, L. V., Abratte, C. M., Schimenti, J. C., Southard, T. L. & Fortier, L. A. Genetic background affects induced pluripotent stem cell generation. *Stem Cell Res. Ther.* **3**, 30 (2012).
50. Azizi, H., Ghasemi Hamidabadi, H. & Skutella, T. Differential Proliferation Effects after Short-Term Cultivation of Mouse Spermatogonial Stem Cells on Different Feeder Layers. *Cell J.* **21**, 186–193 (2019).
51. Choupani, F. *et al.* Feeding role of mouse embryonic fibroblast cells is influenced by genetic background, cell passage and day of isolation. *Zygote* **30**, 550–560 (2022).
52. Cesare, E. *et al.* 3D ECM-rich environment sustains the identity of naive human iPSCs. *Cell Stem Cell* **29**, 1703-1717.e7 (2022).

53. Szczerbinska, I. *et al.* A Chemically Defined Feeder-free System for the Establishment and Maintenance of the Human Naive Pluripotent State. *Stem Cell Rep.* **13**, 612–626 (2019).
54. Puck, T. T., Cieciura, S. J. & Robinson, A. GENETICS OF SOMATIC MAMMALIAN CELLS : III. LONG-TERM CULTIVATION OF EUPLOID CELLS FROM HUMAN AND ANIMAL SUBJECTS. *J. Exp. Med.* **108**, 945–956 (1958).
55. Holmes, R. PREPARATION FROM HUMAN SERUM OF AN ALPHA-ONE PROTEIN WHICH INDUCES THE IMMEDIATE GROWTH OF UNADAPTED CELLS IN VITRO. *J. Cell Biol.* **32**, 297–308 (1967).
56. Hayman, E. G., Pierschbacher, M. D., Suzuki, S. & Ruoslahti, E. Vitronectin--a major cell attachment-promoting protein in fetal bovine serum. *Exp. Cell Res.* **160**, 245–258 (1985).
57. Hayman, E. G., Pierschbacher, M. D., Ohgren, Y. & Ruoslahti, E. Serum spreading factor (vitronectin) is present at the cell surface and in tissues. *Proc. Natl. Acad. Sci.* **80**, 4003–4007 (1983).
58. Hayman, E. G. & Ruoslahti, E. Distribution of fetal bovine serum fibronectin and endogenous rat cell fibronectin in extracellular matrix. *J. Cell Biol.* **83**, 255–259 (1979).
59. Murray, P. *et al.* The self-renewal of mouse embryonic stem cells is regulated by cell–substratum adhesion and cell spreading. *Int. J. Biochem. Cell Biol.* **45**, 2698 (2013).
60. Balbasi, E., Guven, G. & Terzi Cizmecioglu, N. Mouse Embryonic Stem Cell Culture in Serum-Containing or 2i Conditions. in *Embryonic Stem Cell Protocols* (ed. Turksen, K.) 275–294 (Springer US, New York, NY, 2022). doi:10.1007/7651_2021_438.
61. Vallier, L., Alexander, M. & Pedersen, R. A. Activin/Nodal and FGF pathways cooperate to maintain pluripotency of human embryonic stem cells. *J. Cell Sci.* **118**, 4495–4509 (2005).
62. Petrov, P. B., Considine, J. M., Izzi, V. & Naba, A. Matrisome AnalyzeR – a suite of tools to annotate and quantify ECM molecules in big datasets across organisms. *J. Cell Sci.* **136**, jcs261255 (2023).
63. Merkle, F. T. *et al.* Human pluripotent stem cells recurrently acquire and expand dominant negative P53 mutations. *Nature* **545**, 229–233 (2017).
64. Lezmi, E., Jung, J. & Benvenisty, N. High prevalence of acquired cancer-related mutations in 146 human pluripotent stem cell lines and their differentiated derivatives. *Nat. Biotechnol.* 1–5 (2024) doi:10.1038/s41587-023-02090-2.
65. Li, M. M. *et al.* Standards and Guidelines for the Interpretation and Reporting of Sequence Variants in Cancer: A Joint Consensus Recommendation of the Association for Molecular Pathology, American Society of Clinical Oncology, and College of American Pathologists. *J. Mol. Diagn. JMD* **19**, 4 (2017).
66. Bar, S., Schachter, M., Eldar-Geva, T. & Benvenisty, N. Large-Scale Analysis of Loss of Imprinting in Human Pluripotent Stem Cells. *Cell Rep.* **19**, 957–968 (2017).
67. Nazor, K. L. *et al.* Recurrent Variations in DNA Methylation in Human Pluripotent Stem Cells and their Differentiated Derivatives. *Cell Stem Cell* **10**, 620 (2012).
68. Rostovskaya, M., Stirparo, G. G. & Smith, A. Capacitation of human naïve pluripotent stem cells for multi-lineage differentiation. *Dev. Camb. Engl.* **146**, dev172916 (2019).
69. Zhao, C. *et al.* A Comprehensive Human Embryogenesis Reference Tool using Single-Cell RNA-Sequencing Data. 2021.05.07.442980 Preprint at https://doi.org/10.1101/2021.05.07.442980 (2024).
70. Cinkornpumin, J. K. *et al.* Naive Human Embryonic Stem Cells Can Give Rise to Cells with a Trophoblast-like Transcriptome and Methylome. *Stem Cell Rep.* **15**, 198–213 (2020).
71. Rostovskaya, M., Andrews, S., Reik, W. & Rugg-Gunn, P. J. Amniogenesis occurs in two independent waves in primates. *Cell Stem Cell* **29**, 744-759.e6 (2022).
72. Zorzan, I. *et al.* Chemical conversion of human conventional PSCs to TSCs following transient naive gene activation. *EMBO Rep.* **24**, e55235 (2023).
73. Yang, Y. *et al.* Heightened potency of human pluripotent stem cell lines created by transient BMP4 exposure. *Proc. Natl. Acad. Sci.* **112**, E2337–E2346 (2015).
74. Heidari Khoei, H. *et al.* Generating human blastoids modeling blastocyst-stage embryos and implantation. *Nat. Protoc.* **18**, 1584–1620 (2023).
75. Petropoulos, S. *et al.* Single-Cell RNA-Seq Reveals Lineage and X Chromosome Dynamics in Human Preimplantation Embryos. *Cell* **165**, 1012–1026 (2016).

1025 76. Xiang, L. *et al.* A developmental landscape of 3D-cultured human pre-gastrulation embryos.
1026 *Nature* **577**, 537–542 (2020).
1027 77. Meistermann, D. *et al.* Integrated pseudotime analysis of human pre-implantation embryo
1028 single-cell transcriptomes reveals the dynamics of lineage specification. *Cell Stem Cell* **28**,
1029 1625-1640.e6 (2021).
1030 78. Tyser, R. C. V. *et al.* Single-cell transcriptomic characterization of a gastrulating human
1031 embryo. *Nature* **600**, 285–289 (2021).
1032 79. Behringer, R., Gertsenstein, M., Nagy, K. V. & Nagy, A. Testing Serum Batches for Mouse
1033 Embryonic Stem Cell Culture. *Cold Spring Harb. Protoc.* **2017**, pdb.prot092411 (2017).
1034 80. Lazzarano, S. *et al.* Genetic mapping of species differences via in vitro crosses in mouse
1035 embryonic stem cells. *Proc. Natl. Acad. Sci.* **115**, 3680–3685 (2018).
1036 81. Yamanishi, A. *et al.* Collection of homozygous mutant mouse embryonic stem cells arising from
1037 autodiploidization during haploid gene trap mutagenesis. *Nucleic Acids Res.* **46**, e63 (2018).
1038 82. Acosta, S., Fiore, L., Carota, I. A. & Oliver, G. Use of two gRNAs for CRISPR/Cas9 improves
1039 bi-allelic homologous recombination efficiency in mouse embryonic stem cells. *genesis* **56**,
1040 e23212 (2018).
1041 83. Tamura, Y. *et al.* Homologous recombination is reduced in female embryonic stem cells by two
1042 active X chromosomes. *EMBO Rep.* **22**, e52190 (2021).
1043 84. Tsai, L.-K. *et al.* ZSCAN4 interacts with PARP1 to promote DNA repair in mouse embryonic
1044 stem cells. *Cell Biosci.* **13**, 193 (2023).
1045 85. Aflatoonian, B. *et al.* Generation of Sheffield (Shef) human embryonic stem cell lines using a
1046 microdrop culture system. *Vitro Cell. Dev. Biol. - Anim.* **46**, 236–241 (2010).
1047 86. Pantazis, C. B. *et al.* A reference human induced pluripotent stem cell line for large-scale
1048 collaborative studies. *Cell Stem Cell* **29**, 1685-1702.e22 (2022).
1049 87. Okae, H. *et al.* Derivation of Human Trophoblast Stem Cells. *Cell Stem Cell* **22**, 50-63.e6
1050 (2018).
1051 88. Io, S., Iemura, Y. & Takashima, Y. Optimized protocol for naive human pluripotent stem cell-
1052 derived trophoblast induction. *STAR Protoc.* **2**, 100921 (2021).
1053 89. Rivron, N. C. *et al.* Tissue deformation spatially modulates VEGF signaling and angiogenesis.
1054 *Proc. Natl. Acad. Sci. U. S. A.* **109**, 6886–6891 (2012).
1055 90. Pasque, V. *et al.* X Chromosome Reactivation Dynamics Reveal Stages of Reprogramming to
1056 Pluripotency. *Cell* **159**, 1681–1697 (2014).
1057 91. Michalski, A. *et al.* Mass Spectrometry-based Proteomics Using Q Exactive, a High-
1058 performance Benchtop Quadrupole Orbitrap Mass Spectrometer*. *Mol. Cell. Proteomics* **10**,
1059 M111.011015 (2011).
1060 92. Freed, D., Aldana, R., Weber, J. A. & Edwards, J. S. The Sentieon Genomics Tools - A fast and
1061 accurate solution to variant calling from next-generation sequence data. 115717 Preprint at
1062 https://doi.org/10.1101/115717 (2017).
1063 93. McLaren, W. *et al.* The Ensembl Variant Effect Predictor. *Genome Biol.* **17**, 122 (2016).
1064 94. Patro, R., Duggal, G., Love, M. I., Irizarry, R. A. & Kingsford, C. Salmon provides fast and
1065 bias-aware quantification of transcript expression. *Nat. Methods* **14**, 417–419 (2017).
1066 95. Soneson, C., Love, M. I. & Robinson, M. D. Differential analyses for RNA-seq: transcript-level
1067 estimates improve gene-level inferences. Preprint at
1068 https://doi.org/10.12688/f1000research.7563.2 (2016).
1069 96. Robinson, M. D., McCarthy, D. J. & Smyth, G. K. edgeR: a Bioconductor package for
1070 differential expression analysis of digital gene expression data. *Bioinformatics* **26**, 139–140
1071 (2010).
1072 97. Hansen, S. L. *et al.* An organoid-based CRISPR-Cas9 screen for regulators of intestinal
1073 epithelial maturation and cell fate. *Sci. Adv.* **9**, eadg4055 (2023).
1074 98. Hao, Y. *et al.* Integrated analysis of multimodal single-cell data. *Cell* **184**, 3573-3587.e29
1075 (2021).
1076 99. Tirosh, I. *et al.* Dissecting the multicellular ecosystem of metastatic melanoma by single-cell
1077 RNA-seq. *Science* **352**, 189–196 (2016).
1078 100. Marthandan, S. *et al.* Similarities in Gene Expression Profiles during In Vitro Aging of Primary
1079 Human Embryonic Lung and Foreskin Fibroblasts. *BioMed Res. Int.* **2015**, 731938 (2015).

1080 101. Chen, D. *et al.* Transcriptomic profiles of human foreskin fibroblast cells in response to orf
1081 virus. *Oncotarget* **8**, 58668–58685 (2017).
1082 102. Jang, Y. J., Kim, M., Lee, B.-K. & Kim, J. Induction of human trophoblast stem-like cells from
1083 primed pluripotent stem cells. *Proc. Natl. Acad. Sci.* **119**, e2115709119 (2022).
1084 103. Wei, Y. *et al.* Efficient derivation of human trophoblast stem cells from primed pluripotent stem
1085 cells. *Sci. Adv.* **7**, eabf4416 (2021).
1086 104. Zorzan, I. *et al.* The transcriptional regulator ZNF398 mediates pluripotency and epithelial
1087 character downstream of TGF-beta in human PSCs. *Nat. Commun.* **11**, 2364 (2020).
1088 105. Choi, J. *et al.* A comparison of genetically matched cell lines reveals the equivalence of human
1089 iPSCs and ESCs. *Nat. Biotechnol.* **33**, 1173–1181 (2015).
1090 106. Guo, G. *et al.* Epigenetic resetting of human pluripotency. *Development* **144**, 2748–2763 (2017).
1091 107. MacCarthy, C. M. *et al.* Highly cooperative chimeric super-SOX induces naive pluripotency
1092 across species. *Cell Stem Cell* **31**, 127-147.e9 (2024).

1093 **TABLE 1 - Naive hPSC lines used in this study:**

Cell line	Origin	Sex	Derivation	Group
HPD06	Induced from human fibroblasts	Male	Somatic cell reprogramming[30]	Martello
HPD03	Induced from human fibroblasts	Male	Somatic cell reprogramming[30]	Martello
H9[1]	Embryonic	Female	Epigenetic resetting[106]	Leeb
Shef6[85]	Embryonic	Female	Epigenetic resetting[106]	Leeb
H9[1]	Embryonic	Female	Epigenetic resetting[106]	Pasque
SIG-1	Induced from human fibroblasts	Female	mRNA KLF4 reprogramming[27]	Pasque
HNES1	Embryonic	Male	From blastocyst[26]	Pasque
H9[1]	Embryonic	Female	Epigenetic resetting[106]	Zylicz
KOLF2.1J	Induced from human fibroblasts	Male	Episomal Sox2-17 and KLF4 reprogramming[107]	Rivron
SCTi003-A	Induced from human fibroblasts	Female	Episomal Sox2-17 and KLF4 reprogramming[107]	Rivron

1094

FIGURES AND FIGURE LEGENDS

FIGURE 1

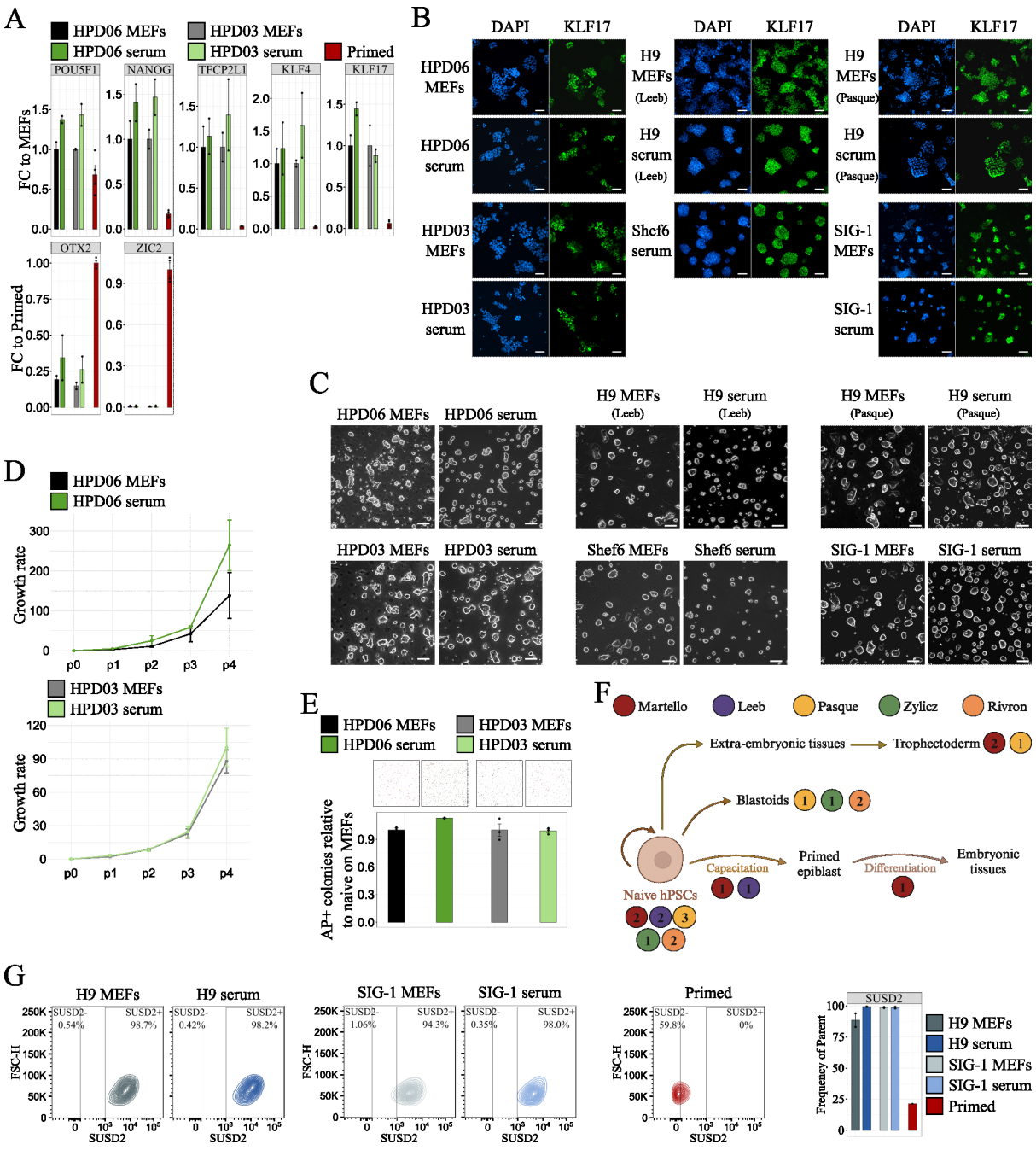

1098 **FIGURE 1 - Serum coating allows for the maintenance of naive hPSCs**

1099 **A** Gene expression analysis by RT-qPCR of general (*POU5F1* and *NANOG*), naive (*TFCP2L1*, *KLF4*
1100 and *KLF17*) and primed (*OTX2* and *ZIC2*) pluripotency markers in HPD06 and HPD03 naive hiPSCs
1101 stably cultured on MEFs, serum or matrigel coating. Bars indicate the mean ± SEM of technical
1102 replicates shown as dots.

1103 **B** Immunostaining for KLF17 of different naive hPSC lines (HPD06, HPD03 and SIG-1 iPSCs, and H9
1104 and Shef6 ESCs) stably cultured on MEFs or serum coating. See also Supplementary Figure 1B-C.
1105 Scale bars: 100 μM.

1106 **C** Morphologies of different naive hPSC lines (HPD06, HPD03 and SIG-1 iPSCs, and H9 and Shef6
1107 ESCs) stably cultured on MEFs or serum coating. Scale bars: 100 μm. Representative images of two
1108 biological replicates.

1109 **D** Growth rate of HPD06 and HPD03 naive hiPSCs stably cultured on MEFs or serum coating. Bars
1110 indicate the mean ± SEM of biological replicates shown as dots.

1111 **E** Top: Representative AP staining images after clonal assay of HPD06 and HPD03 naive hiPSCs stably
1112 cultured on MEFs or serum coating. Bottom: Quantification of the relative number of AP-positive
1113 pluripotent colonies counted per well. Bars indicate the mean ± SEM of biological replicates shown as
1114 dots.

1115 **F** Schematic representation of the analyses performed in this study. Coloured dots identify the
1116 laboratories involved, with numbers indicating cell lines used for each analysis.

1117 **G** Flow cytometry analysis of naive H9 hESCs and SIG-1 hiPSCs stably cultured on MEFs or serum
1118 coating. Left: Contour plots of SUSD2 *versus* forward scatter. Right: Quantification of SUSD2 positive
1119 cells as the frequency of live cells. Bars indicate the mean ± SEM of technical replicates shown as dots.

FIGURE 2

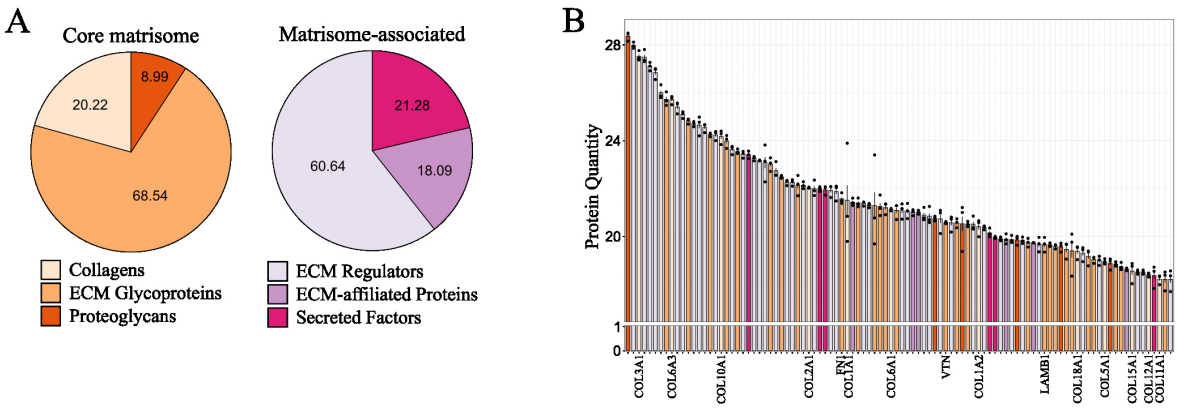

FIGURE 2 - Serum contains a mixture of ECM proteins

A ECM proteins enrichment analysis of the serum coating proteome. Left: Composition of core matrisome proteins expressed in percentage. Right: Composition of matrisome-associated proteins expressed in percentage.

B Top 100 most abundant proteins of the serum coating. Commonly used surface coatings for feeder-free cultures and detected collagens are highlighted. Bars indicate the mean ± SEM of technical replicates shown as dots.

1129 **FIGURE 3**

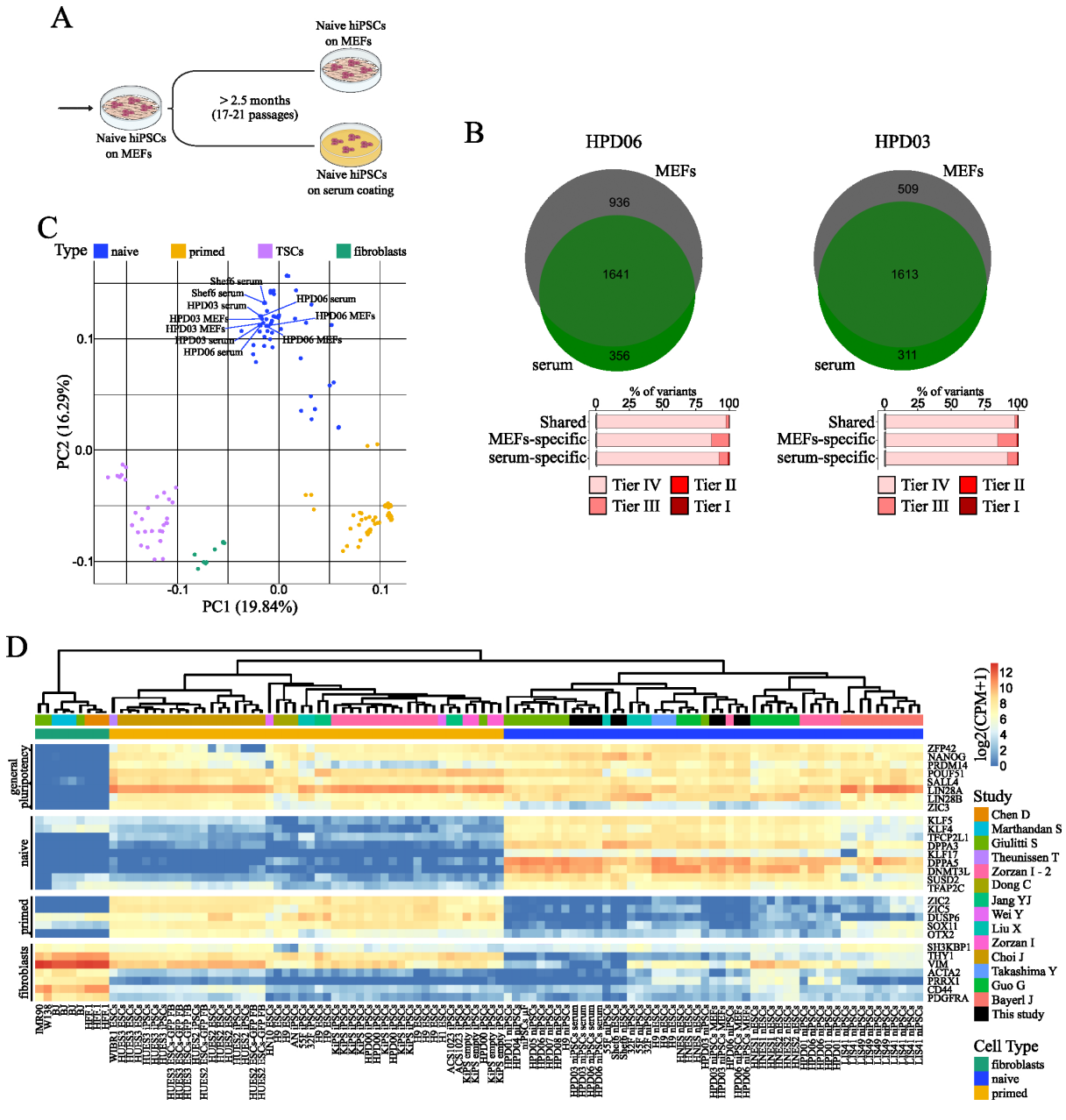

1130

1131 **FIGURE 3 - Naive hPSCs on serum coating do not accumulate pathogenic**
1132 **mutations and maintain their transcriptomic profile**

1133 **A** Schematic representation of the experimental setting for the Exome-Seq analysis of HPD06 and
1134 HPD03 naive hiPSCs stably cultured on MEFs or serum coating.
1135 **B** Analysis of detected genetic variations in coding genes of HPD06 and HPD03 naive hiPSCs stably
1136 cultured on MEFs or serum coating compared to the reference human genome. Top: Venn diagrams
1137 showing the quantification of shared and culture-specific (MEFs or serum coating) detected variants
1138 and mutated genes identified in each condition. All Tier II detected genes and genes identified as
1139 commonly mutated in hPSCs[64] are highlighted. Bottom: Barplots of the composition of shared and
1140 culture-specific (MEFs or serum coating) detected variants classified by Tier and expressed in
1141 percentage.
1142 **C** Principal component analysis of naive hPSC lines (HPD06 and HPD03 hiPSCs, and Shef6 hESCs)
1143 stably cultured on MEFs or serum coating with published naive and primed hPSCs, TSCs and fibroblast
1144 lines performed on the top 5,000 most variable genes identified through RNA-seq.
1145 **D** Heatmap of general pluripotency, naive, primed, and fibroblasts genes in naive hPSC lines (HPD06
1146 and HPD03 hiPSCs, and Shef6 hESCs) stably cultured on MEFs or serum coating and in published
1147 fibroblasts, primed hPSCs and naive hPSCs.

1148 **FIGURE 4**

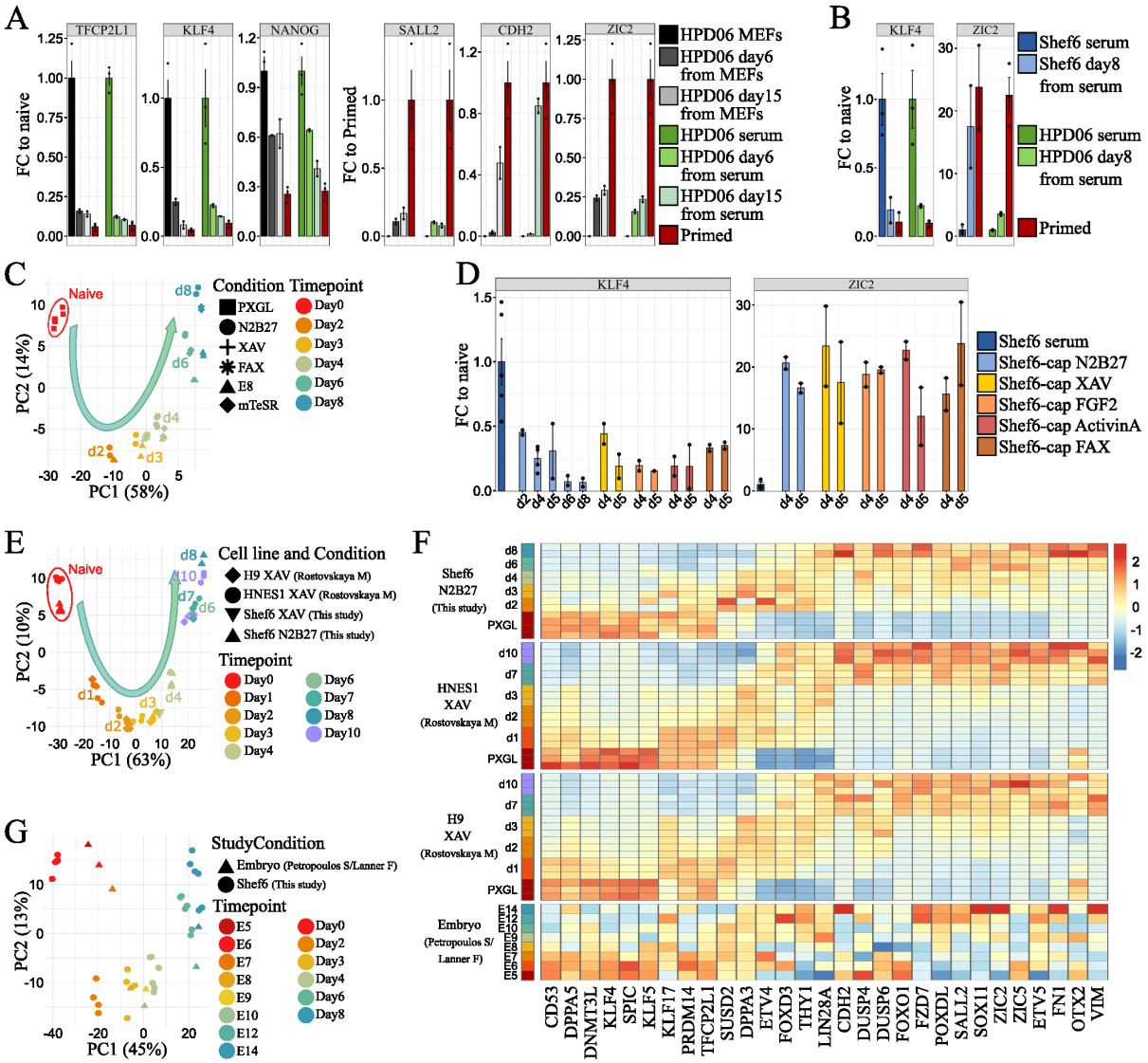

1149

1150 **FIGURE 4 - Feeder-free naive hPSCs can recapitulate embryonic**
1151 **differentiation trajectories**

1152 **A** Gene expression analysis by RT-qPCR of naive (*TFCP2L1* and *KLF4*), general (*NANOG*) and primed
1153 (*SALL2*, *CDH2* and *ZIC2*) pluripotency markers in HDP06 hiPSCs capacitated from naive lines stably
1154 cultured on MEFs or serum coating. Bars indicate the mean ± SEM of technical replicates shown as
1155 dots.
1156 **B** Gene expression analysis by RT-qPCR of naive (*KLF4*) and primed (*ZIC2*) pluripotency markers in
1157 Shef6 hESCs and HDP06 hiPSCs capacitated from naive lines stably cultured on serum coating. Bars
1158 indicate the mean ± SEM of technical replicates shown as dots.
1159 **C** Principal component analysis of all genes identified via RNA-seq of an eight-day differentiation time
1160 course starting from Shef6 naive hESCs stably cultured on serum coating in PXGL. Differentiation was
1161 induced by culture in basal medium (N2B27) with or without supplementation of TNKS1/2 inhibition
1162 (XAV) or FGF2-ActivinA-XAV (FAX) or commercial media containing FGF2 and Activin A
1163 signalling modulators (E8 or mTeSR).
1164 **D** Gene expression analysis by RT-qPCR of naive (*KLF4*) and primed (*ZIC2*) pluripotency markers of
1165 Shef6 naive hESCs stably cultured on serum coating and capacitated in basal medium (N2B27)
1166 supplemented with XAV, FGF2, Activin A or a combination of all three (FAX). Bars indicate the
1167 mean ± SEM of technical replicates shown as dots.
1168 **E** Principal component analysis of the abovementioned feeder-free eight-day differentiation time course
1169 in N2B27 integrated with already published RNA-seq data of H9 and HNES1 hESCs cultured on MEFs
1170 and capacitated in N2B27 supplemented with XAV for up to 10 days[68]. Data was batch-corrected for
1171 data sets.
1172 **F** Heatmaps showing the expression of general pluripotency, naive, and primed markers. *In vitro* data
1173 includes serum-adapted Shef6 naive hESC lines capacitated in N2B27 and published data for H9 and
1174 HNES1 hESCs cultured on MEFs and capacitated in N2B27 supplemented with XAV[68]. The human
1175 embryo reference dataset was a subset for embryonic cells spanning E5-E14[75]. Expression levels for
1176 bulk data are row-wise z-transformed DESeq2-normalized counts. For the embryo data expression
1177 values were normalised, averaged and then log-transformed.
1178 **G** Principal component analysis of the abovementioned feeder-free eight-day differentiation time
1179 course (N2B27, E8 and mTeSR) integrated with pseudo bulk data derived from the human embryo
1180 reference dataset (subset for embryonic cells spanning E5-E14). Data was batch-corrected for data sets
1181 and then filtered by the 9376 DEGs ($|\log2FC| > 1$, $padj < 0.05$) when comparing the naive state with
1182 any of the differentiation conditions and time points.

FIGURE 5

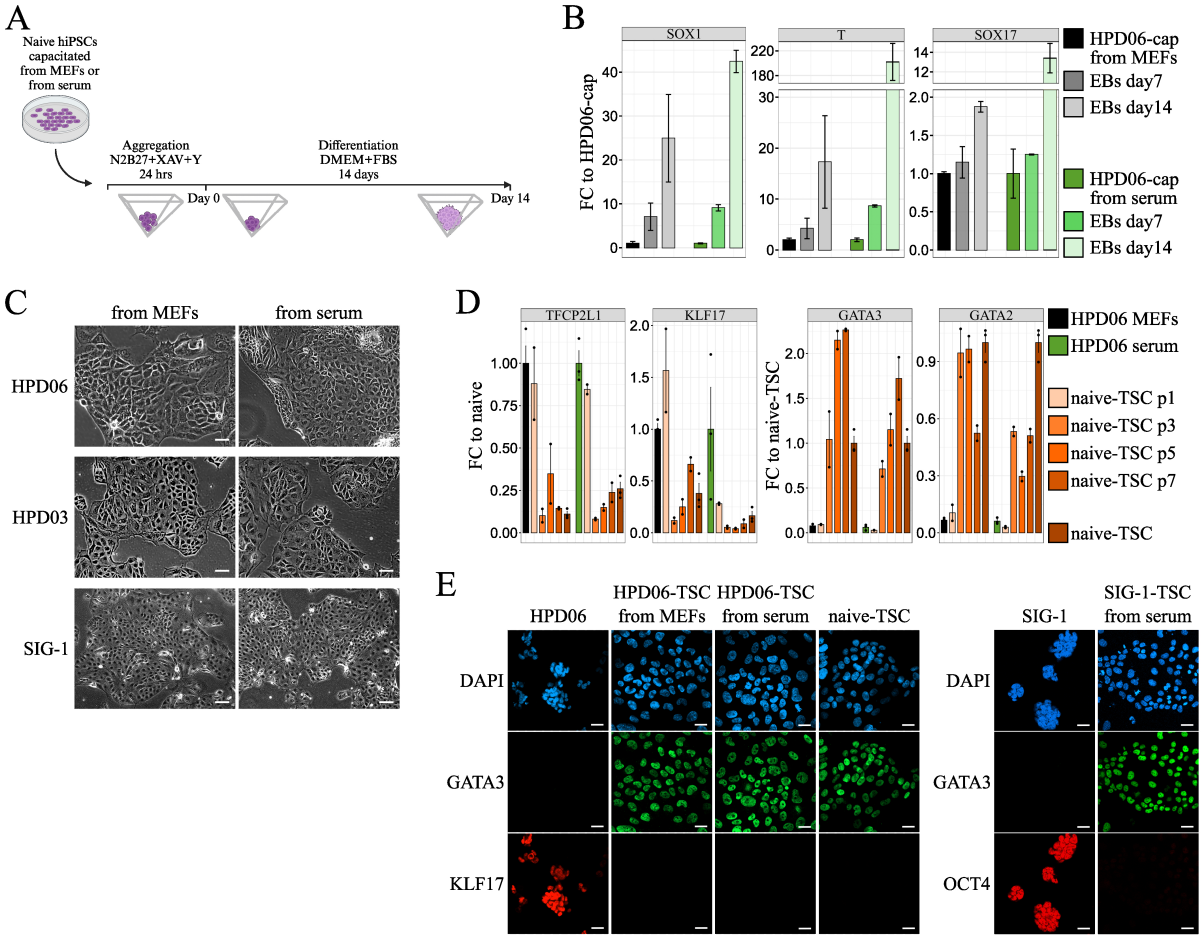
A
Naive hiPSCs capacitated from MEFs or from serum
Aggregation N2B27+XAV+Y 24 hrs
Differentiation DMEM+FBS 14 days
Day 0
Day 14
B
SOX1
T
SOX17
FC to HPD06-cap
HPD06-cap from MEFs
EBs day7
EBs day14
HPD06-cap from serum
EBs day7
EBs day14
C
from MEFs
from serum
HPD06
HPD03
SIG-1
D
TFCP2L1
KLF17
GATA3
GATA2
FC to naive
FC to naive-TSC
HPD06 MEFs
HPD06 serum
naive-TSC p1
naive-TSC p3
naive-TSC p5
naive-TSC p7
naive-TSC
E
HPD06
HPD06-TSC from MEFs
HPD06-TSC from serum
naive-TSC
SIG-1
SIG-1-TSC from serum
DAPI
GATA3
KLF17
OCT4

1185 **FIGURE 5 - Feeder-free naive hPSCs efficiently differentiate to embryonic**
1186 **and extraembryonic lineages**

1187 **A** Morphologies of EBs derived from capacitated HPD06 naive hiPSCs stably cultured on MEFs or
1188 serum coating. Red dashed circles highlight outgrowths. Red dashed lines highlight EBs outgrowths.
1189 Scale bars: 100 µm. Representative images of two biological replicates.
1190 **B** Gene expression analysis by RT-qPCR of germ layers markers (*SOX1*, *T*, and *SOX17*) in EBs derived
1191 from capacitated HPD06 naive hiPSCs stably cultured on MEFs or serum coating. Bars indicate the
1192 mean ± SEM of technical replicates shown as dots.
1193 **C** Morphologies of TSCs derived from HPD06, HPD03 and SIG-1 naive hiPSCs stably cultured on
1194 MEFs or serum coating. Scale bars: 50 µm. Representative images of two biological replicates.
1195 Representative images of two biological replicates.
1196 **D** Gene expression analysis by RT-qPCR of naive pluripotency (*TFCP2L1* and *KLF17*) and TSCs
1197 (*GATA3* and *GATA2*) markers in TSCs derived from HPD06 naive hiPSCs stably cultured on MEFs or
1198 serum coating. Bars indicate the mean ± SEM of technical replicates shown as dots.
1199 **E** Immunostaining for TSCs (GATA3) and naive (KLF17) or general pluripotency (OCT4) markers of
1200 trophectoderm derived from HPD06 and SIG-1 naive hiPSCs stably cultured on MEFs or serum coating.
1201 Scale bars: 50 µM. Representative images of two independent experiments are shown.

FIGURE 6

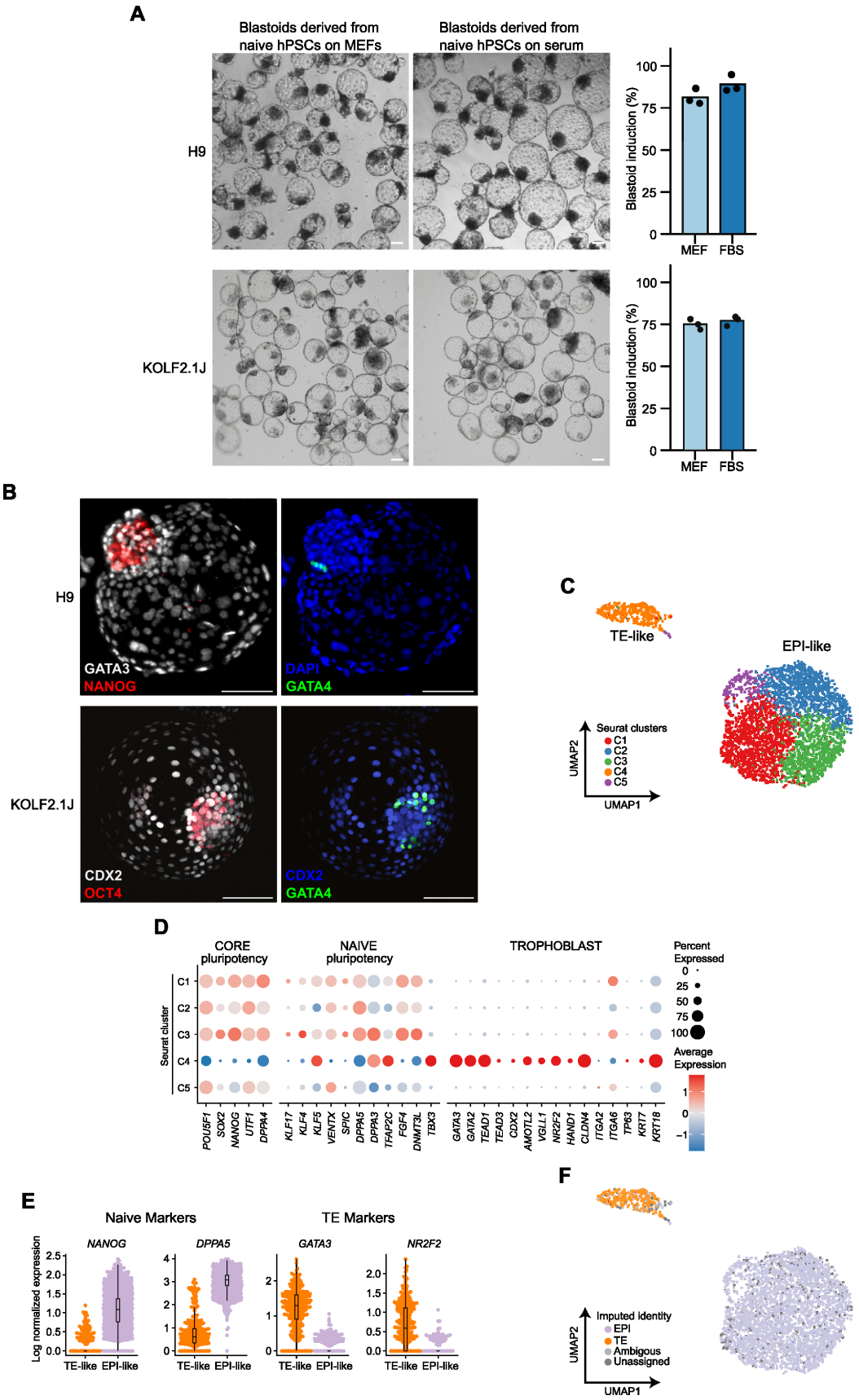
A
Blastoids derived from naive hPSCs on MEFs
Blastoids derived from naive hPSCs on serum
H9
KOLF2.1J
Blastoid induction (%)
MEF
FBS
B
GATA3
NANOG
DAPI
GATA4
CDX2
OCT4
C
TE-like
EPI-like
Seurat clusters
C1
C2
C3
C4
C5
UMAP2
UMAP1
D
CORE pluripotency
NAIVE pluripotency
TROPHOBLAST
Percent Expressed
Average Expression
Seurat cluster
POU5F1
SOX2
NANOG
UTF1
DPPA4
KLF17
KLF4
KLF5
VENTX
SPIC
DPPA5
DPPA3
TFAP2C
FGF4
DNMT3L
TBX3
GATA3
GATA2
TEAD1
TEAD3
CDX2
AMOTL2
VGLL1
NR2F2
HAND1
CLDN4
ITGA2
ITGA6
TP63
KRT7
KRT18
E
Naive Markers
TE Markers
NANOG
DPPA5
GATA3
NR2F2
Log normalized expression
TE-like
EPI-like
F
Imputed Identity
EPI
TE
Ambigous
Unassigned
UMAP2
UMAP1

1204 **FIGURE 6 - Feeder-free naive hPSCs efficiently form blastoids**

1205 **A** Left: brightfield images of blastoids induced from naive H9 hESC and naive KOLF2.1J hiPSCs
1206 cultured on MEFs or serum coating. Scale bar: 100 µm. Right: quantification of induction efficiency
1207 from naive H9 hESC and naive KOLF2.1J hiPSCs cultured on MEFs or serum-coated dishes. Data is
1208 based on brightfield images of d5 blastoids. Data is presented as the mean and data points of 3 biological
1209 replicates.

1210 **B** Immunostaining of d5 blastoids derived from naive H9 hESC and naive KOLF2.1J hiPSCs cultured
1211 on serum coating. Blastoids were stained for TE (GATA3 or CDX2), PrE (GATA4) and EPI (NANOG
1212 and OCT4) markers. Shown is the maximum projection. Scale bars: 100 µm.

1213 **C** UMAP plot from scRNA-seq analysis of blastoids from naive H9 hESCs cultured on serum coating.
1214 Cells are coloured according to the sample Seurat cluster (n = 3260). Highlighted are TE-like (cluster
1215 4) and EPI-like clusters.

1216 **D** Expression of selected lineage-specific marker genes across Seurat clusters from (C). The size of the
1217 dots represents the proportion of cells in the indicated group expressing the given gene and colour
1218 encodes the scaled average expression.

1219 **E** Combined beeswarm and box plots of gene expression of naive pluripotency markers (*NANOG* and
1220 *DPPA5*) and TE markers (*GATA3* and *NR2F2*) from (C). Cells were separated based on their EPI or TE
1221 signature. Single cells are plotted as dots; boxes span the interquartile range (IQR), the centre line
1222 indicates the median and whiskers extend to values within 1.5 times the IQR.

1223 **F** UMAP plots as in (C) but with cells based on the imputed annotation of *in vitro* samples from a
1224 reference in vivo dataset[69]. Unassigned and ambiguous labels refer to cells with either none or with
1225 more than two imputed annotations respectively.

1226 **SUPPLEMENTARY MATERIAL**

1227 **SUPPLEMENTARY TABLE 1 - Primers used in this study:**

Group	Target	Sequence
Martello Group	POU5F1_FW POU5F1_RW	GTGGAGGAAGCTGACAACAA ATTCTCCAGGTTGCCTCTCA
	NANOG_FW NANOG_RV	CAAAGGCAAACAACCCACTT TCTGCTGGAGGCTGAGGTAT
	TFCP2L1_FW TFCP2L1_RW	GGAGTTCCAGCCATGCTCTT CCTGCTTGAAGATGGGCAGA
	KLF4 _FW KLF4 _RV	CCCAATTACCCATCCTTCCT CAGGTGTGCCTTGAGATGG
	KLF17_FW KLF17_RV	CACACAGGTGAGAGGCCATA ACTCGGTGTGTACCCGCATA
	OTX2_FW OTX2_RV	GAGAGGAGGTGGCACTGAAA TGACCTCCATTCTGCTGTTG
	ZIC2_FW ZIC2_RV	CATGCACGTCCACACCTC CTCATGGACCTTCATGTGCTT
	SALL2_FW SALL2_RV	GCACGAATCCGAGAGGAG TCACCATTACAGGAGGGTCAG
	CDH2_FW CDH2_RV	CGTGGTCAAACCAATCGAC AACAGACACGGTTGCAGTTG
	GATA3_FW GATA3_RV	ACAGAAGGCAGGGAGTGTGT TCCGTTCATTTTGTGATAGAGC
	GATA2_FW GATA2_RV	GACTACAGCAGCGGACTCTT GCCTTCTGAACAGGAACGAG
	IGFBP3_FW IGFBP3_RV	CCTGCCGTAGAGAAATGGAA AAGGGCGACACTGCTTTTT
	BAMBI_FW BAMBI_RV	GAGGCCTCAGGACAAGGAAA CCCGGAACCACAACTCTTT
	SOX1_FW SOX1_RV	GCTGACACCAGACTTGGGTTT CCCCTCGAGCAAAGAAAACG
	T_FW T_RV	GCCAGATCATGCTGAACTCC AAGCTTTTGCAAATGGATTGT
	SOX17_FW SOX17_RV	ACGCCGAGTTGAGCAAGA TCTGCCTCCTCCACGAAG
	GAPDH_FW GAPDH_RV	GCCTCAAGATCATCAGCAATGC CGCCACAGTTTCCCGGAG
Leeb group	KLF4_FW KLF4_RV	CCCACATGAAGCGACTTCCC CAGGTCCAGGAGATCGTTGAA
	ZIC2_FW ZIC2_RV	CATGCACGGTCCACACCTC CTCATGGACCTTCATGTGCTT
	ACTB_FW ACTB_RV	CCAACCGCCGAGAAGATGA CCAGCGGCGTACAGGGATAG

1228

1229 **SUPPLEMENTARY TABLE 2 - Primary antibodies used in this study:**

Group	Target	Conjugate	Supplier	Catalog ID	IF dil.
Martello Group	KLF17	-	Atlas Antibodies	HPA024629	1:250
	OCT4 (C-10)	-	Santa Cruz	sc-5279	1:300
	NANOG	-	Cell Signaling	D73G4	1:100
	TFCP2L1	-	R&D Systems	AF5726	1:250
	GATA3	-	R&D Systems	AF2605	1:100
Leeb Group	KLF17	-	Atlas Antibodies	HPA024629	1:333
	OCT4 (C-10)	-	Santa Cruz	sc5279	1:50
	SUSD2 (W5C5)	APC	BioLegend	327408	1:100
Pasque Group	KLF17	-	Abcam	HPA024629	1:300
	OCT4 (C-10)	-	Santa Cruz	sc-5279	1:100
	NANOG	-	BD Bioscience	560482	1:50
	GATA3		R&D System	AF2605	1:100
	SOX17	-	R&D System	AF1924	1:100
	SUSD2	PE	Biolegend	327406	1:50
	GATA2	-	Sigma-Aldrich	WH0002624M1	1:100
	NANOG	-	Abcam	ab21624	1:100
Zylicz Group	NANOG	-	Abcam	ab173368	1:250
	GATA3	-	Abcam	ab199428	1:250
	GATA4	-	eBioscience	14-9980-80	1:250
Rivron Lab	OCT4 (C-10)	-	Santa Cruz	sc-5279	1:200
	CDX2	-	Abcam	ab76541	1:1000
	GATA4	-	Invitrogen	14-9980-82	1:400

1230

1231 **SUPPLEMENTARY FIGURE 1**

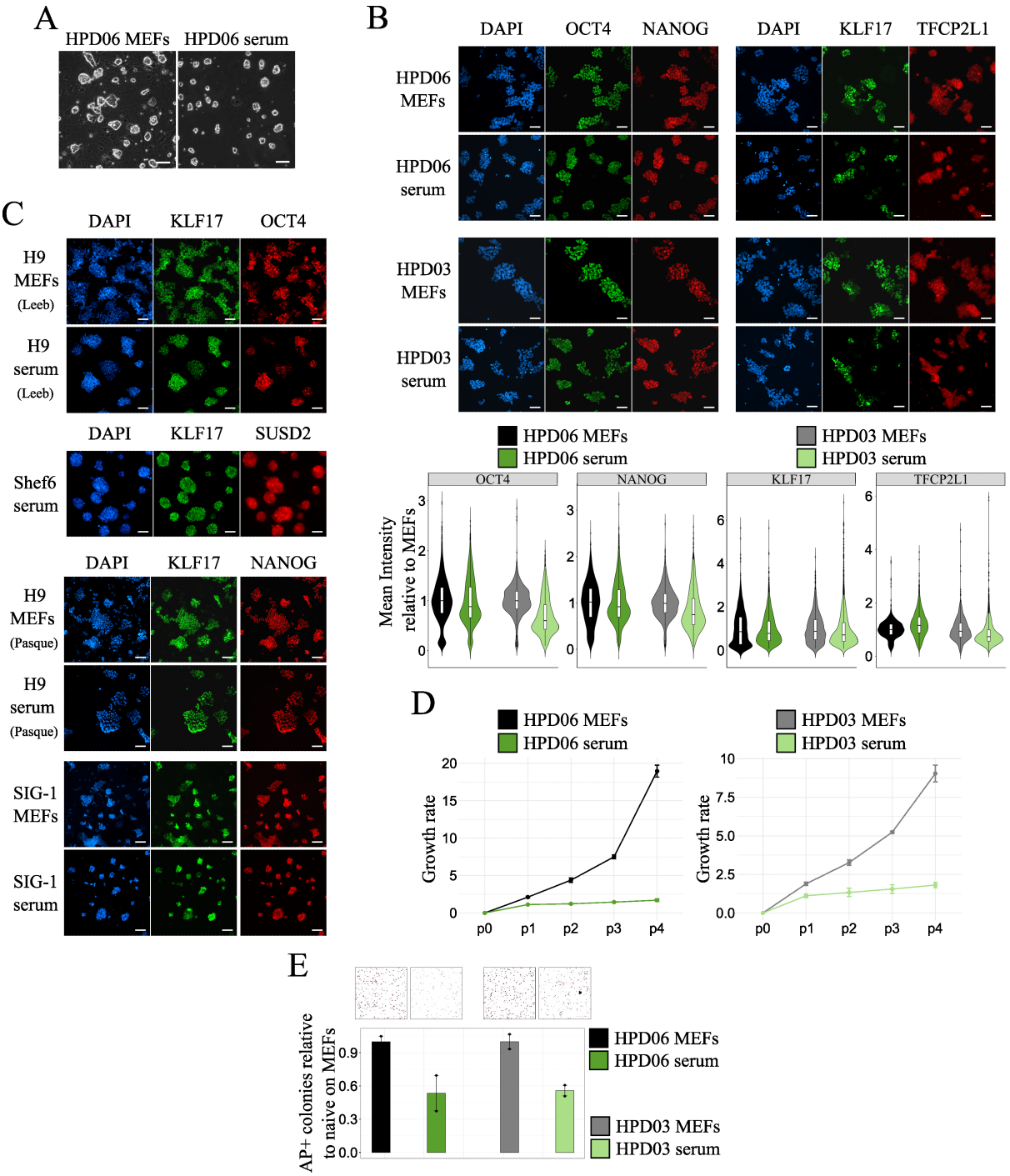

1232

1233 # SUPPLEMENTARY FIGURE 1

1234 **A** Morphologies of HPD06 naive hiPSC line cultured on MEFs or serum coating when plated at a low
1235 density at the 4th passage. Scale bars: 100 µm. Representative images of two biological replicates.
1236 **B** Top: Immunostaining for general pluripotency (OCT4 and NANOG) and naive (KLF17 and
1237 TFCP2L1) markers of HPD06 and HPD03 naive hiPSCs cultured on MEFs or serum coating at the 4th
1238 passage. Complete view of Figure 1B. Scale bars: 100 µM. Representative images of two independent
1239 experiments are shown. Bottom: Mean fluorescence intensity quantification for general pluripotency
1240 (OCT4 and NANOG) and naive (KLF17 and TFCP2L1) markers of HPD06 and HPD03 naive hiPSCs
1241 cultured on MEFs or serum coating at the 4th passage. At least 700 nuclei from five randomly selected
1242 fields from two independent experiments were analysed for each condition. The box plot indicates the
1243 25th, 50th and 75th percentiles.
1244 **C** Immunostaining for general pluripotency (OCT4 and NANOG) and naive (KLF17 and SUSD2)
1245 markers of H9 and Shef6 naive hESCs, and SIG-1 hiPSCs stably cultured on MEFs or serum coating.
1246 Complete view of Figure 1B. Scale bars: 100 µM.
1247 **D** Growth rate of HPD06 and HPD03 naive hiPSCs cultured on MEFs or serum coating when plated at
1248 a low density over the first 4 passages of the conversion. Bars indicate the mean ± SEM of biological
1249 replicates shown as dots.
1250 **E** Top: Representative AP staining images after clonal assay of HPD06 and HPD03 naive hiPSCs
1251 cultured on MEFs or serum coating when plated at a low density at the 4th passage. Bottom:
1252 Quantification of the relative number of AP-positive pluripotent colonies counted per well. Bars
1253 indicate the mean ± SEM of biological replicates shown as dots.

SUPPLEMENTARY FIGURE 2

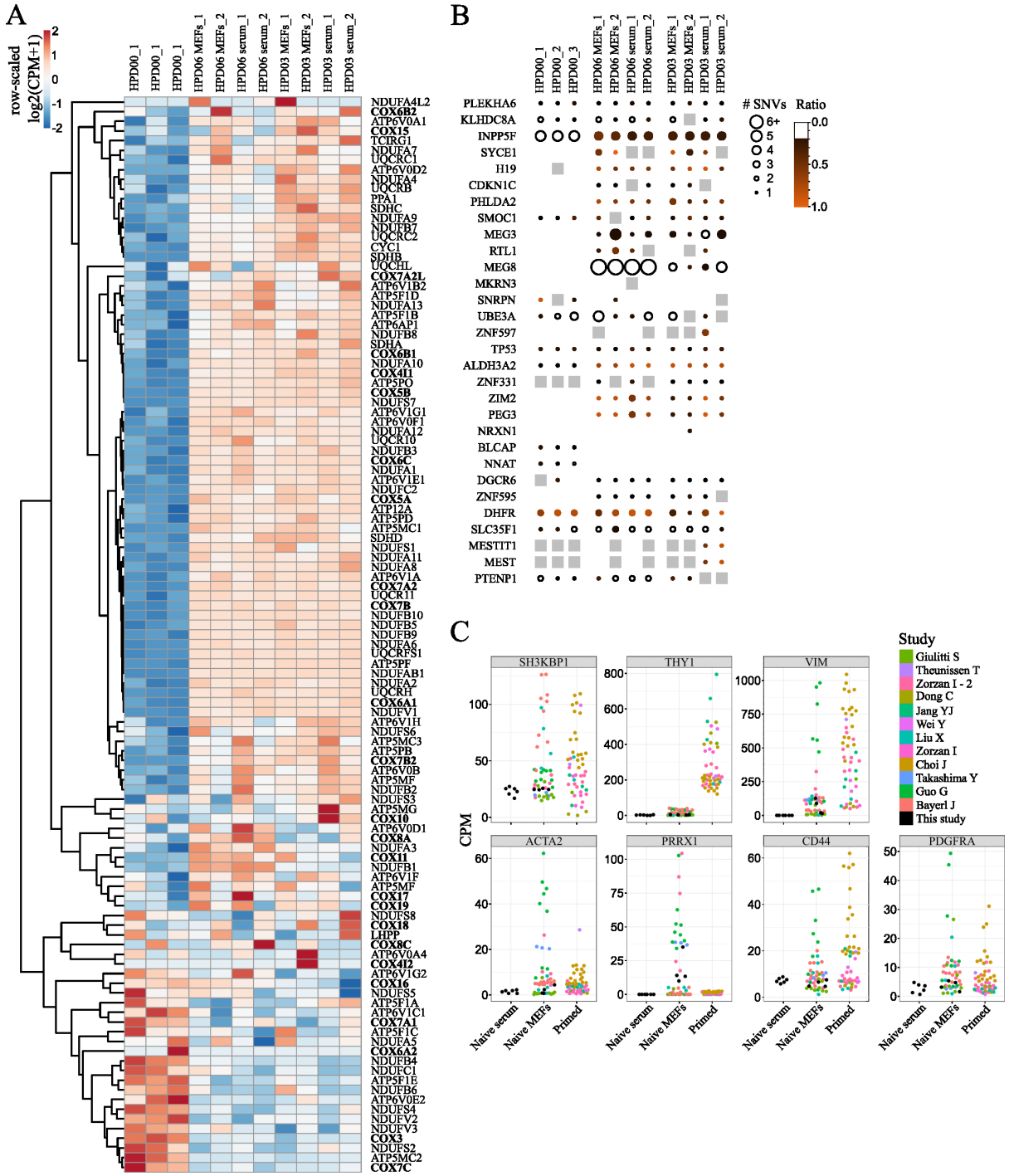

1256 **SUPPLEMENTARY FIGURE 2**

1257 **A** Heatmap of oxidative phosphorylation genes from the KEGG PATHWAY Database
1258 (https://www.genome.jp/kegg/pathway.html) and COX genes[24] in HPD00 primed hiPSCs and HPD06
1259 and HPD03 naive hiPSCs stably cultured on MEFs or serum coating.
1260 **B** BrewerIX gene summary panel results on RNA-Seq data from HPD00 primed hiPSCs and HPD06
1261 and HPD03 naive hiPSCs stably cultured on MEFs or serum coating. Empty dots indicate detected
1262 genes with no evidence of biallelic expression, grey squares indicate genes detected but not reaching
1263 the thresholds, and the absence of any symbol indicates that the gene was not detected.
1264 **C** Absolute expression (CPM) of fibroblasts markers from Figure 2D in naive hPSC lines (HPD06 and
1265 HPD03 hiPSCs, and Shef6 hESCs) stably cultured on MEFs or serum coating and in published naive
1266 hPSCs on MEFs and primed hPSCs.

SUPPLEMENTARY FIGURE 3

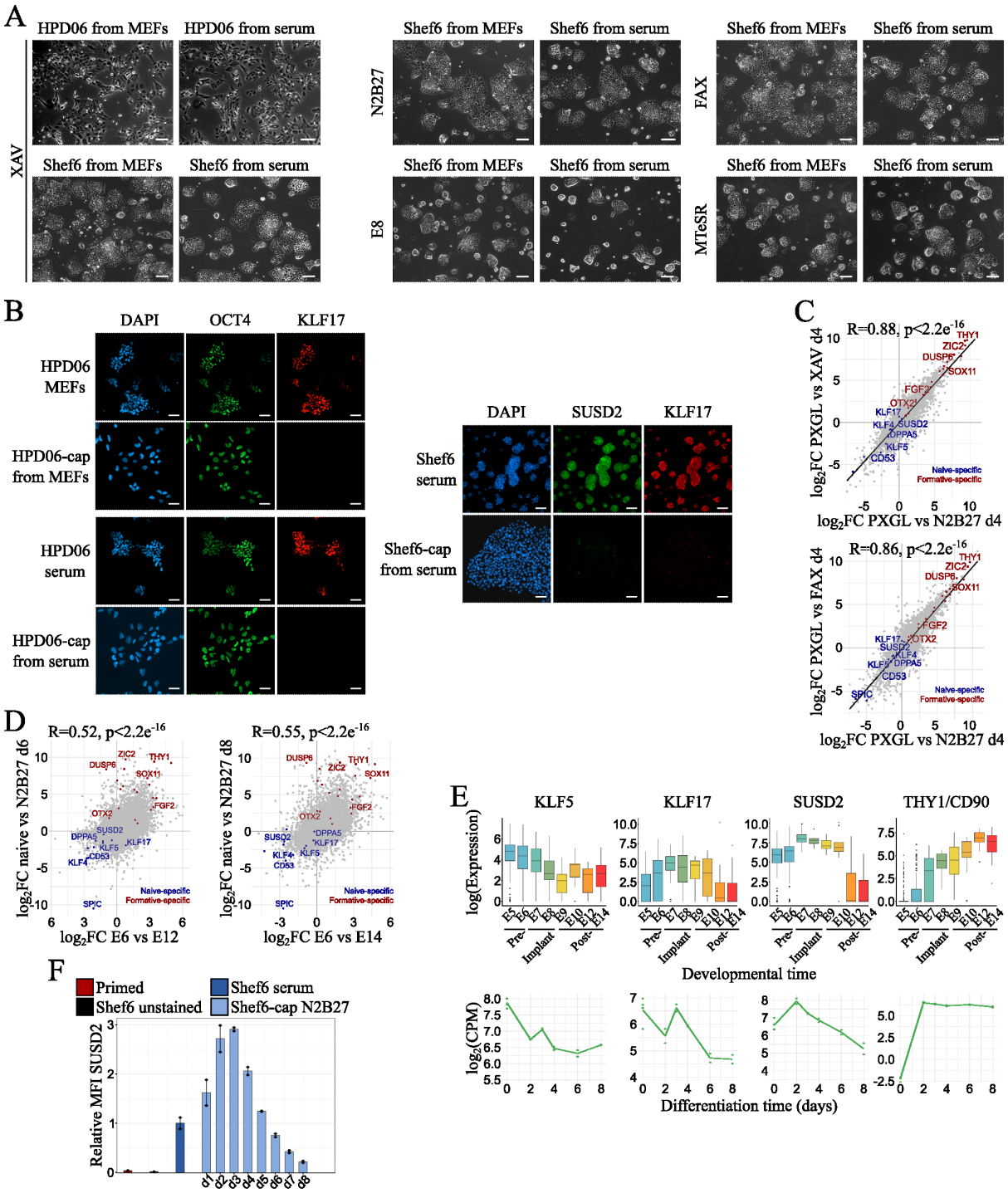

1269 # SUPPLEMENTARY FIGURE 3

1270 **A** Morphologies of HPD06 hiPSCs and Shef6 hESCs capacitated from naive lines stably cultured on
1271 MEFs or serum coating under different media compositions. Scale bars: 100 µm. Representative images
1272 of two biological replicates.
1273 **B** Immunostaining for general (OCT4) and naive (KLF17 and SUSD2) pluripotency markers of HPD06
1274 hiPSCs and Shef6 hESCs capacitated from naive lines stably cultured on MEFs or serum coating. Scale
1275 bars: 100 µM. Representative images of two biological replicates.
1276 **C** Scatter Plots showing log2 fold changes (log2FC) of Shef6 naive hESCs stably cultured on serum
1277 coating differentiated for 4 days in unsupplemented N2B27, N2B27 supplemented with XAV, or
1278 N2B27 supplemented with XAV, FGF2, and Activin A (FAX) compared to the naive state. Data was
1279 filtered for the 9376 DEGs ($|\log2FC| > 1$, $padj < 0.05$) identified in any comparison with the naive state.
1280 Spearman correlation (R) and p-values are overlaid, with a linear regression line fitted. Selected naive-
1281 and primed-specific markers are labelled.
1282 **D** Scatter Plots showing log2 fold changes (log2FC) of Shef6 naive hESCs stably cultured on serum
1283 coating in the naive state versus differentiation for 6 or 8 days in N2B27, compared to corresponding
1284 developmental times (E6 vs. E12 or E14) from the human embryonic reference dataset (subset for
1285 embryonic lineages only)[75]. Spearman correlation (R) and p-values are overlaid, with selected naive-
1286 and primed-specific genes labelled.
1287 **E** Gene expression of naive (*KLF5*, *KLF17* and *SUSD2*), and primed (*THY1*) pluripotency markers in
1288 the human embryonic reference dataset (subset for embryonic lineages only)[75] and for Shef6 naive
1289 hESCs stably cultured on serum coating differentiated for 6-8 days in N2B27. Lines indicate inferred
1290 trends based on mean values, with technical replicates shown as dots.
1291 **F** Relative median fluorescence intensity (MFI) of the naive-specific surface marker SUSD2 in Shef6
1292 naive hESCs stably cultured on serum coating during capacitation for 8 days in N2B27, measured by
1293 flow cytometry. Bars represent the mean ± SEM of technical replicates shown as dots.

1294 **SUPPLEMENTARY FIGURE 4**

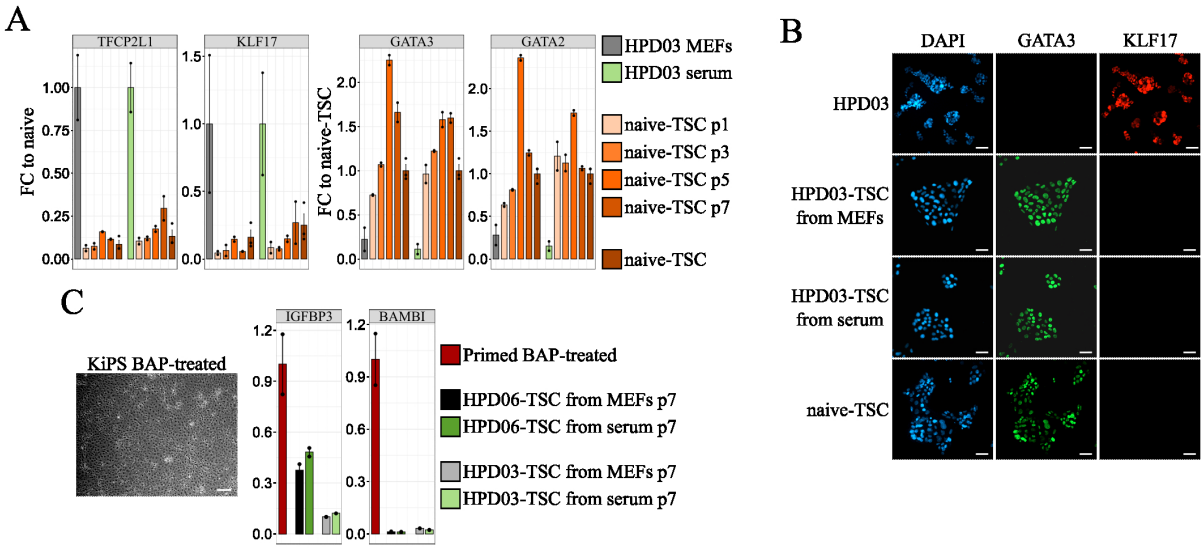

1295

1296 **SUPPLEMENTARY FIGURE 4**

1297 **A** Gene expression analysis by RT-qPCR of naive pluripotency (*TFCP2L1* and *KLF17*) and TSCs
1298 (*GATA3* and *GATA2*) markers in TSCs derived from HPD03 naive hiPSCs stably cultured on MEFs or
1299 serum coating. Bars indicate the mean ± SEM of technical replicates shown as dots.
1300 **B** Immunostaining for TSCs (GATA3) and naive pluripotency (KLF17) markers in TSCs derived from
1301 HPD03 naive hiPSCs stably cultured on MEFs or serum coating. Scale bars: 100 µM. Representative
1302 images of two independent experiments are shown.
1303 **C** Left: Morphology of KiPS primed hiPSCs treated with BAP medium for 4 days. Scale bar: 100 µm.
1304 Right: Gene expression analysis by RT-qPCR of amnion markers (*IGFBP3* and *BAMBI*) in TSCs
1305 derived from HPD06 and HPD03 naive hiPSCs stably cultured on MEFs or serum coating. Bars indicate
1306 the mean ± SEM of technical replicates shown as dots.

SUPPLEMENTARY FIGURE 5

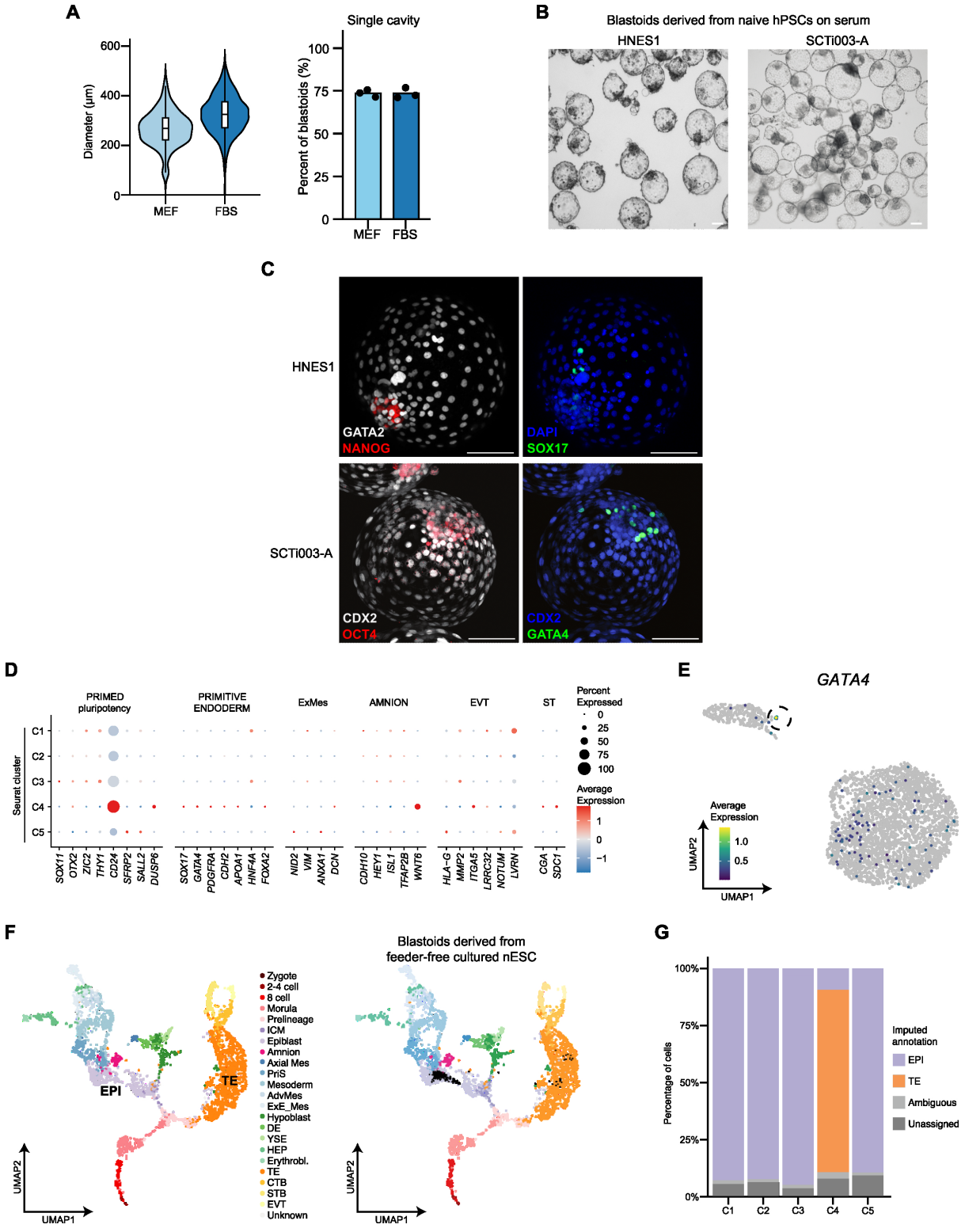

1309 # SUPPLEMENTARY FIGURE 5

1310 **A** Quantification of blastoid diameter (left) and blastoids with a single cavity (right) in structures formed
1311 from naive H9 hESCs cultured on MEFs or serum coating. Left: data is presented as violin plots with
1312 the median, 25, 75 percentiles (± min-max) of n = 407 (MEFs) and 806 (serum coating) across 3
1313 biological replicates. Right: Data shows the mean percentages and data points of 3 biological replicates.
1314 **B** Brightfield images of blastoids induced from naive HNES1 hESC and naive SCTi003-A hiPSCs
1315 cultured on serum coating. Scale bar: 100 µm.
1316 **C** Immunostaining of blastoids derived from naive HNES1 hESC and naive SCTi003-A hiPSCs
1317 cultured on serum coating. Blastoids were stained for TE (GATA2 or CDX2), PrE (GATA4 or SOX17)
1318 and EPI (NANOG and OCT4) markers. Shown is the maximum projection. Scale bars: 100 µm.
1319 **D** Expression of selected lineage-specific marker genes across Seurat clusters from Figure 6C. The size
1320 of the dots represents the proportion of cells in the indicated group expressing the given gene and colour
1321 encodes the scaled average expression.
1322 **E** UMAP plot from scRNA-seq analysis as in Figure 6C. Cells are coloured according to *GATA4*
1323 expression (n = 3260).
1324 **F** (left) UMAP of human pre-implantation and post-implantation embryos with annotation for scRNA-
1325 seq data integration from[69] with cells coloured by cell type. (right) Projection of in vivo reference data
1326 with in vitro d5 blastoids from naive H9 hESC cultured on serum coating. Black dots show
1327 neighbourhoods of in vitro generated cells projected onto a reference UMAP.
1328 **G** Imputed cell annotation across different Seurat clusters as in Figure 6F. Unassigned and ambiguous
1329 labels refer to cells with either none or with more than two imputed stages respectively.